Characterization of Low Velocity Impact Damage in Metallic Honeycomb Sandwich Aircraft Panels using Finite Element Analysis

Caractérisation des dommages dus aux impacts à basse vitesse sur les panneaux sandwichs en nid d'abeille à peaux métalliques en utilisant une analyse par éléments finis

A Thesis Submitted to the Division of Graduate Studies of the
Royal Military College of Canada
by

Lt(N) Gregory C. Clarke, BSc

In Partial Fulfillment of the Requirement for the Degree of
Master of Applied Science, Mechanical Engineering

December 2017

This thesis is dedicated to my loving wife Amanda. Without her patience and support, nothing would have been accomplished.

Acknowledgements

I would like to thank my supervisors, Dr. Diane Wowk and Dr. Catharine Marsden, as well as Dr. Billy Allan for their guidance and support during the conduct of this research and the writing of this thesis.

Also, I would like to thank Mr. Tyler Reyno, Mr. Joel Benotto, Capt. Stephen Prior and Mr. Tanner Rellinger for their insight and for providing a good "sounding board" when I needed one.

Abstract

Honeycomb sandwich panels are used as structural elements for applications requiring high strength and bending stiffness to weight ratios, such as many aircraft structures. Metallic types are most widely found on older fleets of aircraft. These panels are highly susceptible to impact damage due to the low out of plane stiffness of the core and the thin face sheets. Unfortunately, the extent of damage to the core is not easily determined via visual inspection. Current literature on honeycomb panel impact damage is focused on surface dents and the planar area of underlying core damage, with little focus on the depth to which damage extends.

Using the finite element analysis software ANSYS, simulations were conducted for a wide range of impacts, with differing panel and impactor characteristics. It was found that for low velocity impacts on panels of the same core density that the depth to which the damage extends is constant for any size of dent. It was also determined that the width of the damage to the core matched the width of the residual dent and that the panel thickness did not affect surface or core damage unless the panel was so thin that the core underneath the impact area was thoroughly crushed.

Keywords: honeycomb sandwich structures, surface damage, core damage, low-velocity impact, impact damage, aluminum honeycomb, dent, finite element analysis

Résumé

Les panneaux sandwichs en nid d'abeille sont utilisés comme des éléments structuraux pour les applications nécessitant des rapports de résistance et de rigidité à la flexion élevés par rapport au poids. Les panneaux à peaux métalliques sont plus répandus dans les structures des flottes d'avions plus anciennes. Ces panneaux sont très susceptibles de subir des dommages d'impact à cause de la faible rigidité hors plan de l'âme et des peaux minces. Malheureusement, l'étendue des dommages causés à l'âme n'est pas facilement déterminée par une inspection visuelle. La littérature récente sur les dommages causés aux panneaux en nid d'abeilles est axée sur les empreintes superficielles et la surface endommagée à l'âme sous-jacente avec peu d'attention sur la profondeur de l'empreinte.

En utilisant le logiciel d'analyse par éléments finis ANSYS, des simulations ont été effectuées pour un large éventail d'impacts, avec différentes caractéristiques de panneaux et des modes d'impact. Elles ont démontré que, pour des impacts à basse vitesse sur des panneaux en nids d'abeille de même densité, la profondeur à laquelle les dommages s'étendent est constante pour n'importe quelle taille d'empreinte. Il a également été constaté que la largeur des dommages au nid d'abeille correspond à la largeur de l'empreinte résiduelle et que l'épaisseur du panneau n'affectait pas les dommages de surface ou de l'âme à moins que le panneau soit si mince que l'âme sous la zone d'impact était complètement écrasée.

Mots-clés: Panneaux sandwichs en nid d'abeille, dommage à la surface, dommage au nid d'abeille, impact à basse vitesse, dommage dû à un impact, nid d'abeille à peaux d'aluminium, empreinte, méthode des éléments finis.

Contents

List of Figures

List of Tables

List of Acronyms

BVID	Barely Visible Impact Damage
CAI	Compression After Impact
CFRP	Carbon Fibre Reinforced Polymers
FAA	Federal Aviation Administration (of the United States of America)
FEA	Finite Element Analysis
RAM	Random Access Memory
RCAF	Royal Canadian Air Force
SPH	Smooth Particle Hydrodynamics
SRM	Structural Repair Manual
VID	Visible Impact Damage

List of Symbols

L	In-plane length of honeycomb core section, along ribbon axis
T	Out-of-plane thickness of honeycomb core section
TM	Trademark Symbol
W	In-plane width of honeycomb core section, across ribbon axis

1. Introduction

Sandwich panels are widely used in structural applications requiring a high bending stiffness and low weight and are commonly found in the aerospace industry. They consist of two thin face sheets on either side of a lightweight core material. The face sheets are designed to carry the bulk of the bending load, with the core carrying the shear load and maintaining the separation of the face sheets. One of the primary drawbacks of these structures is their susceptibility to impact damage. The honeycomb structure is easily damaged when the face sheets are impacted even at low energy levels and this damage can negatively affect the residual strength of the panel. Metallic sandwich panels, where both the face sheet and the honeycomb core are made of aluminum are used throughout the Bell CH-146 Griffon, currently used by the Royal Canadian Air Force (RCAF) for Search and Rescue, Surveillance and Reconnaissance and Tactical Air Support missions.

1.1. Motivation

Structural repair manuals (SRM) for the Griffon helicopter specify the amount of damage that can exist in honeycomb sandwich panels before they need to be repaired or replaced. Observations made in the field by personnel working with the aircraft have indicated that these allowable damage limits, which will be discussed further in Section 2.8, may be quite conservative in nature. The RCAF is interested in examining the damage limits for the honeycomb panels on the Griffon helicopter with the intention of relaxing the limits based on a better understanding of the expected damage and the effect of this damage on the residual strength. This thesis is part of a larger project that aims to develop a finite element modelling methodology that can be used to predict the residual strength of metallic honeycomb sandwich panels subject to low-velocity impact damage. Accurately modelling the residual strength of an impacted panel first requires detailed knowledge of the damage that is caused to the face sheets and the core.

Non-destructive testing methods for quantifying impact damage, which will be discussed further in Section 2.6, are typically only capable of measuring the depth and length of surface dents and the planar damage area of the underlying honeycomb core. They are unable to determine the depth to which the damage extends in the core and destructive sectioning of the panel is currently the only method for determining this metric.

1.2. Goals and Scope

There are two main goals of this thesis. The first goal is to determine the mode, size and severity of the damage that is expected in different panel configurations when subjected to different impact scenarios. The second goal is to determine what relationships exist between the subsurface damage and the size and shape of the residual dents in the face sheets. Particular attention is paid to the depth to which the damage extends into the core. The focus will be on low-velocity impacts that produce damage that is less than or near the allowable damage limits.

Dynamic finite element simulations that consider contact, plasticity and material failure were conducted in order to accomplish these goals. Variations in impactor mass, impactor velocity, impactor stiffness, face sheet thickness, core density and panel thickness were examined, with a total of 65 impact simulations conducted.

1.3. Outline

Chapter 2 provides an overview of the nature of sandwich panels, how they are affected by impacts and an examination of the literature pertaining to experimental testing and numerical simulations of impacts and their effect upon the post-impact structural characteristics of the panel. **Chapter 3** describes the details of the finite element simulations that were conducted in order to create different damage states in the panels. **Chapter 4** discusses the simulation results, including relationships between different panel and impact parameters and the resulting damage. **Chapter**

5 elaborates on these results and explains the physical mechanisms responsible for the trends observed in Chapter 4. **Chapter 6** summarizes the findings of the thesis and provides recommendations on areas for future research.

2. Literature Review

This chapter provides an overview of sandwich aircraft panels and their usage and response to impact events. Previous research that has been conducted to understand low-velocity impact events, the detection and measurement of impact damage and parameters that affect the degree or type of damage caused in sandwich panels is also presented. Different modelling techniques for simulating impact response are discussed as well as areas for which there is an overall lack of research in this field.

2.1. Sandwich Panel Overview

The main components of a sandwich panel are the face sheets, the core and the adhesive that bonds them together, as shown in Figure 2-1. Within the aerospace industry, aluminum or carbon fiber reinforced polymer are the most commonly used materials for the face sheets of sandwich panels. The core is typically made of foam or honeycomb structures made of aramid paper (e.g. Nomex™), or aluminum. According to Aktay, Johnson and Kröplin [1], aluminum honeycombs are falling out of use in favour of Nomex™ due to its relatively high susceptibility to corrosion in the face of moisture ingress.

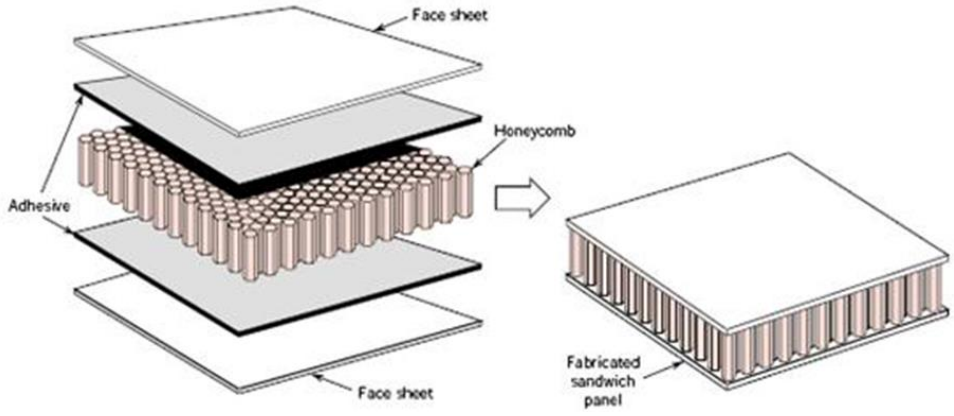

Figure 2-1: Honeycomb sandwich panel construction [2]

In the case of aluminum honeycombs, the core is typically constructed by one of two methods. The expansion method involves stacking sheets of aluminum foil of the appropriate thickness together in sequence and applying an adhesive in lines such that when expanded, the sections that were adhered together form one set of parallel cell walls in the honeycomb structure [3]. Figure 2-2 illustrates this process.

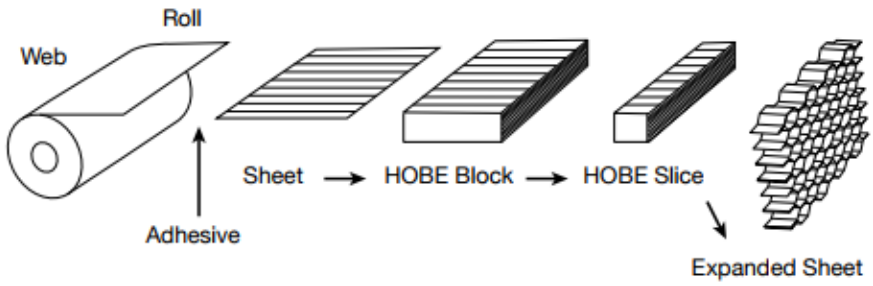

Figure 2-2: Expansion honeycomb core manufacturing method [3]

An alternative method involves feeding a roll of aluminum foil through a corrugated roller, creating a corrugated sheet. Adhesive is applied to the flat sections of this sheet and sections of corrugated sheets are stacked with the flats held together and the adhesive is cured. This is typically performed for honeycomb cores with a smaller cell size than those made via the expansion process. Figure 2-3 illustrates this process. Both methods involve the creation of a honeycomb structure where the cell walls along one orientation have double the wall thickness as compared to those in either oblique orientation (plus or minus 60° for a hexagonal core), as a result of bonding together two sheets of aluminum foil. This orientation is referred to as the "ribbon direction" or the L direction as indicated in Figure 2-3.

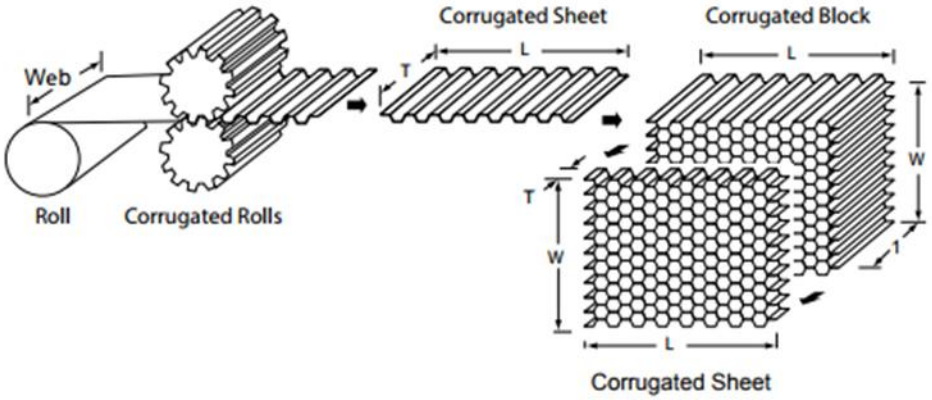

Figure 2-3: Corrugation honeycomb core manufacturing method [3]

Sandwich panels are constructed by attaching the face sheets to the core material with an adhesive. In the case of carbon fibre reinforced polymers (CFRP) or other composite material face sheets, this may occur concurrently with the curing process for the composite material.

2.2. Low-Velocity Impact

Unlike high velocity (e.g. hail strikes), ballistic (e.g. small arms fire), or hypervelocity impacts (e.g. space debris), low-velocity impacts are typically characterized as having contact durations long enough that the stress and shock waves caused by the impact reach the boundaries of the panel before the contact with the impacting body has finished. Feraboli [4] outlined how it is not the velocity per se that is often the determining factor in whether or not an impact is considered to be low velocity, but rather the ratio of the mass of the impactor to the mass of the panel being tested. A ratio of at least 10:1 is sufficient to be considered low-velocity. Low-velocity impacts have a tendency to cause damage which can be difficult to detect using visual inspection methods, as compared to the deeper dents or punctures caused by impacts at higher velocities, as discussed by Prior [5]. This makes them of particular interest, as low-velocity impacts can result in

reductions in structural stiffness and strength which can go unnoticed during normal inspection routines and could possibly lead to in-flight structural failures.

Consideration of such damage, termed barely visible impact damage (BVID) is a critical component of a damage tolerant design philosophy, which is used as part of the certification process. The Federal Aviation Administration (FAA) of the United States defines BVID as damage at the threshold of reliable detection [6]. Boeing considers dents in the 0.25 to 0.5 mm depth range to be the threshold for BVID [7].

2.3. Damage Tolerant Design and Visible Impact Damage

The key aspects of damage tolerant design are as follows [8]:

- "Acceptance that damage will occur";
- "An adequate system of inspection so the damage may be detected"; and
- "An adequate strength maintained in the damaged structure"

Damage tolerance includes both the residual strength and damage propagation requirements of design. A structure must be designed such that any BVID which could occur in the structure would not impair the residual strength of the aircraft such that it would fail under the ultimate load (defined as a 1.5 times safety factor of the largest load [limit load] the aircraft is expected to experience during its service life), nor would the damage from BVID propagate to the point that it could do so before it would be detected during normal inspection routines [6].

BVID caused by low-velocity impacts can still have significant effects on the residual stiffness and strength of a sandwich panel. Raju *et al.* [9] showed reductions in compressive strength of up to 60% caused by BVID impacts in some panels.

Conversely, visible impact damage (VID) includes any damage which "can be reliably detected by scheduled or directed field inspections performed at specified intervals" [6]. VID must not propagate such that it would grow to the point of reducing the residual strength of the structure below the limit load level (vice the ultimate load requirement for BVID) before repair. Therefore, whether or not a repair is mandated when VID is detected depends upon the degree of damage which was caused by the impact and the expected propagation characteristics of that damage.

In the case of a honeycomb sandwich panel, determining the degree to which VID has affected the residual strength requires an accurate assessment of both the amount of damage to the sandwich panel's face sheets and the nature of the damage to the underlying honeycomb core. The ultimate goal of this research is to allow for a more accurate assessment of the effect that VID (within or near the allowable damage limits) has upon the residual strength of honeycomb sandwich panels, when the dent size, shape and distribution on a particular panel is known.

2.4. Impact Damage Mechanism

A typical impact event involves three distinct stages;

a) Initial contact between impactor and face sheet. The face sheet starts to bend as the point of contact is displaced downwards. The honeycomb core starts to deform as well, although it may not be experiencing any permanent damage at this point.

b) Continued downward displacement, until point of maximum indentation. The impactor continues downward until it stops, because all the kinetic energy has been absorbed by the structure. Depending upon the bending stiffness of the face sheet and the shape of the impactor, this may cause a sharp indentation, or the deformation may be smoother and spread over a wider area [10]. During this denting process, the honeycomb core underneath absorbs some of the impact energy and in the process is damaged, via localized folding of the walls, which continues to progressive crumpling and crushing. This may lead to fracture or cracking of the core.

c) Impactor bouncing and face sheet spring-back. The elastic strain energy built up in the impactor and the face sheet releases, transforming back into kinetic energy, pushing the impactor away from the face sheet, at a reduced velocity from the initial impact. The face sheet springs back to its residual dent position as this elastic strain energy is released, resulting in a final dent shape which is less deep than the position of maximum indentation during the impact. The spring back of the face sheet can induce residual tensile loads in the honeycomb core because of the larger degree of plastic deformation that is present in the core. This phenomenon may not occur in the event that the core experienced cracking or fracture, or if disbond occurred due to adhesive failure between the face sheet and core.

2.5. Damage in Panels

The literature covers research on CFRP and Nomex™ sandwich panels far more thoroughly than it does metallic honeycomb sandwich panels. This is likely due to the emerging nature of the technologies involved. There is a natural inclination for researchers to want to focus their efforts on the "cutting edge" materials being use in the latest generations of aircraft. The increasing prevalence of composite materials also coincided with the introduction of efficient Finite Element Analysis (FEA) software packages. As a result, there has been relatively little research focusing on aluminum-aluminum sandwich panels, especially using finite element methods.

2.5.1. Damage Modes in Aluminum – Aluminum Honeycomb Sandwich Panels

2.5.1.1. Aluminum Face Sheet Damage

Research investigating impacts on sandwich panels with aluminum face sheets all observed a residual dent indicating plasticity in the skin [11 – 21]. The size and shape of the resultant dent can have a major impact upon its residual strength, as the load carrying capacity of a thin sheet is reduced based upon factors such as the depth, width, length and placement of the dent [22]. These parameters which have an impact on the load carrying capacity of one of the face sheets will also have an impact on the load

carrying capacity of the sandwich panel as a whole. Puncture or tearing in the face sheet can be caused by sharp impactors, high energy impacts, or some combination thereof [17]. This type of damage will cause stress concentrations around the puncture site which affects the load carrying ability of the face sheet and can also serve as an initiation site for crack growth. The bulk of current literature focuses on impacts which do not result in punctures or cracks in the face sheet.

2.5.1.2. Aluminum Honeycomb Core Damage

Metallic honeycomb core in general exhibits a progressive crushing pattern. The initial downward deflection of the top of the core causes the cell walls to deform laterally, showing increasing wave-like patterns of deflection, until one or more of the lobes of the buckling pattern becomes severe enough to cause a fold in the cell wall. Further compression of the honeycomb core deepens these plastic hinges until the sections of the cell wall above and below the fold make contact, after which another lobe will form and deepen immediately underneath the initial crushed section. Yamashita and Gotoh [23] outlined how this behaviour will continue progressively until the whole core is crushed, as shown in Figure 2-4. Figure 2-5 shows a cross section of a section of honeycomb core where this progressive crushing has occurred, underneath a deep dent.

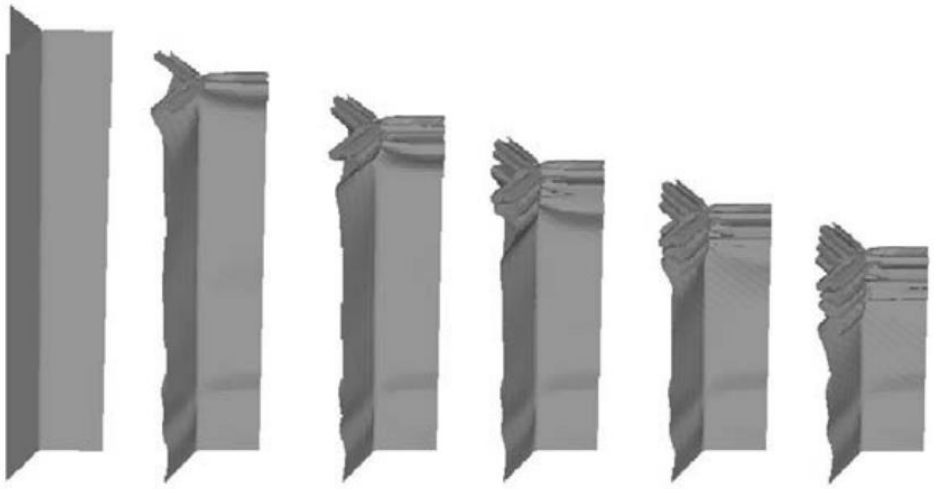

Figure 2-4: Progressive crushing behaviour of a section of honeycomb core [Adapted from Reference 23]

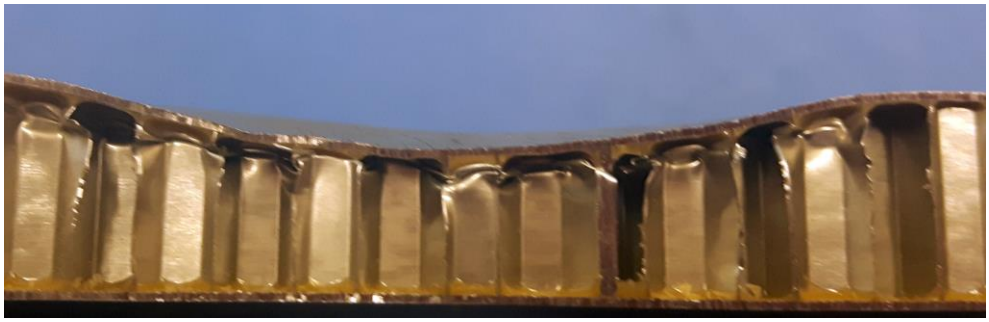

Figure 2-5: Cross section of honeycomb core showing progressive crushing behaviour

Crumpling of the aluminum honeycomb core reduces its effective stiffness and reduces the degree to which the honeycomb core supports the face sheets. This can lead to local wrinkling failure of the face sheet when the panel is loaded in bending or in compression. Once crumpling has initiated, there is a sharp reduction in the maximum load the honeycomb core can carry before crumpling progresses further [3, 24]. Figure 2-6 shows a comparison between the crushing load response of a honeycomb core with and without one pre-deformed end, in which a small section of one

end of the honeycomb core has been manually crumpled prior to flatwise crushing. Without the straight undeformed structure to initially take the load, no peak in load carrying capacity above the average load forms upon initiation of crushing.

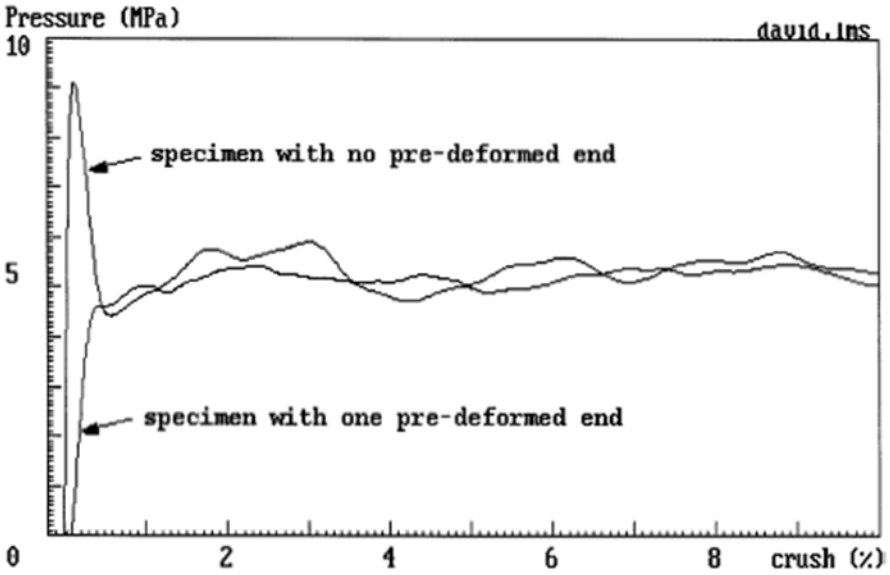

Figure 2-6: Comparison of out-of-plane crushing load for honeycomb core with and without a pre-deformed end [24]

Severe crumpling can cause cracking or fracture within the cell walls of the honeycomb core, which will change the way that loads are transmitted through the panel. This mode of damage can also contribute to wrinkling failure as well as increased stresses in the face sheet.

2.5.1.3. Adhesive Failure

An integral component of a sandwich panel is the adhesive which provides the structural bond between the core and the face sheets. Impacts can cause failure or debonding of this adhesive which results in the core and face sheet separating, as observed by Prior [5]. This type of failure is often seen in regions of the aircraft that are exposed to high temperatures that may degrade the adhesive, or when water egress occurs [25]. The unsupported

face sheet in the dent region is prone to local wrinkling when the panel is loaded in compression or in bending. The cracks in the adhesive that initiate in the dent region may propagate under fatigue loading and could result in large regions of the face sheet separating from the core.

2.5.2. Damage Modes in Non-Metallic Honeycomb Panels

2.5.2.1. Composite Face Sheet Damage

When impacted, face sheets made from composite material such as CFRP may produce damage modes that do not occur in aluminum. This includes fibre breakage, fibre pull-out, delamination between layers, matrix cracking and cross-ply cracks. Of these, one of the most concerning is delamination, as it can be difficult to detect using non-destructive testing methods, it can reduce the strength and stiffness of the panel and has the potential to propagate over a larger area. CFRPs in particular have a tendency towards larger amounts of dent relaxation than metallic face sheets. In some cases the dent can completely spring back, leaving no visible indication that the impact occurred. This was commonly seen in experiments conducted by Tomblin *et al.* [26] and McQuigg *et al.* [27].

2.5.2.2. Non-Metallic Honeycomb Core Damage

Nomex™ honeycomb cores crush and crumple in a similar fashion as aluminum but have higher tendency to fail via brittle fracture. Failure often also typically happens simultaneously throughout the depth of the core, whereas damage to aluminum honeycomb cores is progressive in nature, starting from the impacted face sheet and continuing downwards as the indentation progresses [28]. Nomex™ cores also recover their shape more readily than aluminum after buckling which can increase the tendency towards spring-back of the face sheet [10].

2.6. Impact Damage Detection

Visual inspection is the most common method of initially identifying impact damage to honeycomb sandwich panels. As visual inspection relies upon detecting residual dents, it is more difficult to detect damage to

sandwich panels when significant relaxation of the face sheet occurs. Large subsurface damage areas can exist that would not be detected during a visual inspection, which is especially a problem when the impact is caused by an object with a large radius or with composite face sheets. The generally accepted threshold for what is determined to be BVID is a residual indentation depth of 1.27 mm (0.05") [29], although lower values are used by some [7].

Tomblin *et al.* [26] conducted a series of tests on a number of different configurations of CFRP sandwich panels, using a 25.4 mm (1 inch) and a 76.2 mm (3 inch) diameter impactor. The impacts with the larger impactor rarely caused visible damage, even at energy levels that produced severe damage when the smaller impactor was used. Similar results were observed by Prior [5] in testing on panels with aluminum honeycomb cores and CFRP face sheets. Difficulties with visual detection occur more often in sandwich panels with CFRP face sheets, as impacts on aluminum face sheets leave a residual dent. One technique that has been developed to combat this effect is the creation of a paint system which incorporates microcapsules with a pigment of a different colour, which can leave a visual indication of impact damage on a CFRP face sheet which may otherwise not have any visual signs of the impact. [30]

Impact damage in the core can be detected using tap testing, in which lightly striking the panel with an object can reveal damage due to the resultant change in localized stiffness. The change in the sound created by the tapping is most frequently used by maintenance personnel in the field to detect damage, requiring experienced maintainers with a trained ear for the tonal differences between damaged and undamaged areas. The localized stiffness also affects the contact duration, which was used by Prior [5] to build a damage map. Through Transmission Ultrasonic C-Scan measurements can detect underlying damage by detecting the changes in the propagation of sound waves through a crushed honeycomb core, as was used by Tomblin *et al.* [26] to detect damage, even in instances where complete springback of the face sheets left no residual dent.

Other NDT methods commonly used include thermography, which measures the effect that damage has upon the rate of heat transfer through

a panel; shearography, which detects defects using variations in the reflection of a laser off the surface of a panel, before and after a load is applied to it; radiography, which uses x-ray imaging to provide a detailed view of the interior of a honeycomb panel [5]; 3D laser scanning, which can be used to measure surface damage including dent profiles and eddy current testing which can be used at different frequencies to both measure surface and subsurface damage [31]. These techniques can be used to detect the presence of damage, but none can reliably differentiate between different types of damage, such as cracking, crumpling, or disbond of the core and none can tell the depth or severity of the core damage.

2.7. Impact Damage Characterization

Impact damage to a honeycomb sandwich panel is typically characterized in terms of residual dent depth, dent width or area and planar damage area of damage to the core [26].

Tomblin *et al.* [26] examined the planar cross section of the underlying core damage via C-Scan measurements and visual inspection of the dent in the face sheets, assessing the degree of damage to the face sheet against a qualitative scale. McQuigg *et al.* [27] used visual assessment after destructive sectioning to measure the depth and width of both facesheet and honeycomb core damage. Prior [5] used a combination of visual assessments, tap testing, ultrasonic and x-ray inspection and laser topography to determine the dent depth and the dent and core damage planar area. Reyno *et al.* [31, 32] used laser topography and eddy current testing to determine the depth and planar area of residual surface damage and visual inspection after destructive testing to determine honeycomb core damage width and depth. For determining damage to a honeycomb core cross section, visual inspection was used rather than measuring plastic strain. This thesis aims to evaluate impact damage on metallic honeycomb panels in terms of residual dent depth and width and core damage depth and width.

2.8. Allowable Limits

As part of the damage tolerant design philosophy, aircraft structures will have a certain level of damage that can occur without an immediate repair requirement. These allowable limits can be complex; for impact damage the structural repair manual for the Griffon helicopter [33] outlines different allowable limits on the basis of planar surface area, width, placement and grouping of dents. Some damage is considered negligible, with no requirement to report said damage and no limits upon the number of negligible dents allowed on a panel, such as dents less than 12.7 mm (0.5") wide without any punctures in the skin. Other damage can be considered allowable, which may mean that a single larger dent is allowed (up to 101.6 mm [4"] and 20% of the thickness of the panel deep), or that there will be a limit on the total surface area of the panel covered in smaller dents (20%). Detection and measurement of the area of dents is done visually, with the depth being determined using a manual depth gauge. The current limits are considered by maintenance personnel to be quite conservative, as panels that are retired from service due to these limits still maintain a large degree of their residual strength and stiffness [34].

2.9. Variables Influencing Impact Damage

Much of the literature presents the results of impact testing in terms of contact force history plots. These results are often used as a method of assessing the accuracy of finite element models or as an assessment of the energy absorbed during the impact. Aktay, Johnson and Holzapfel [35] developed a finite element model for a high velocity impact test of two types of composite sandwich panels, one with a foam core and one with a Nomex™ honeycomb core. Their results present a comparison of the contact force history plots between their simulations and the corresponding experimental data. The damage itself was not quantified or compared. Other examples of a similar approach are prevalent in the literature [1, 15, 28, 36 – 38], where experimental or simulated impacts were performed, but quantification of the damage state in the skin and the core was not presented.

2.9.1. Effect on Face Sheet Damage

The tests conducted by Tomblin *et al.* [26] on carbon fibre reinforced polymer panels with Nomex™ honeycomb cores found that that increasing impact energy caused more damage in face sheets, but using a larger impactor (76.2 mm diameter) caused less apparent damage than the smaller impactor (25.4 mm) at equivalent impact energies, in some cases causing no visibly apparent damage at all. Foo, Seah and Chai [20] conducted a series of five experimental impact tests on an aluminum – aluminum honeycomb panels and found a linear relationship between the maximum downward deflection of the impactor (and thus also the impacted face sheet) and the kinetic energy of the impactor. Zhang *et al.* [19] conducted analysis involving a numerical 3D model considering the individual cell walls of the honeycomb core and came to the conclusion that maximum indentation depth increased in a non-linear fashion with regard to impact energy.

Foo, Seah and Chai [20] also conducted a series of finite element simulations using finite element methods to investigate the effect that changing the density of the honeycomb core had upon the damage caused to a face sheet by the impact. They found that a denser core resulted in a smaller damage profile.

Wowk and Marsden [39] conducted FEA simulations of an aluminum-aluminum honeycomb sandwich panel using an impactor with an imposed constant-displacement. Varying the face sheet thickness, they found that the increased stiffness of the thicker face sheet caused the residual dent width to increase linearly with face sheet thickness.

2.9.2. Effect on Honeycomb Core Damage

Tomblin *et al.* [26] also found that despite the aforementioned decrease in apparent face sheet damage when using a larger impactor, the planar area of the underlying damage to the honeycomb core grew with the impactor diameter. Foo, Seah and Chai's [20] set of simulations found that the width of the damaged area of the honeycomb core matched that of the damage in the face sheet.

Horrigan and Aitken [40] found that in one instance, using a hard-bodied impactor, the depth of the damage to the honeycomb core followed the profile of the residual dent. Using a soft-bodied impactor they found that the depth of the damage to the honeycomb core was constant across the damage area. McQuigg *et al.* [27] conducted impact testing and while it was not the focus of their research, they did state that it was "also interesting to note that the depth of the core crush region beneath the indented face sheet stays about the same for all levels of the impact energy". Both Horrigan and Aitken [40] and McQuigg *et al.* [27] were examining composite face sheets bonded to a Nomex™ core.

2.9.3. Effect on Energy Absorption

Foo, Seah and Chai's [20] set of simulations found that changing the density of the honeycomb core had no influence on the amount of energy absorbed during the impact.

Both Zhang *et al.* [18] & Ashab *et al.* [41] concluded that the percentage of energy absorbed by the panel did not vary significantly with impact energy, for impacts within the low-velocity range.

This thesis aims to examine a wider range of impact parameters than have been studied in the literature and to quantify the damage in the face sheets and the core. The focus will be on determining the relationship between different impact and panel parameters and the measureable damage characteristics of dent depth, dent width, core damage depth and core damage width. As FEA will be used, this study is not limited only to visible methods of detecting damage; however, it will not attempt to use measurements which would be impossible to measure in an physical panel, such as stress distribution.

2.10. Finite Element Modelling Techniques

There are two general methods of modelling a honeycomb sandwich panel. One can approximate the structure of the honeycomb within the panel as some other idealized structure, or one can fully model the individual cell

walls. The former approach can in many cases significantly reduce simulation run-times, while sacrificing being able to more accurately model the actual damage mechanism for the damage in the honeycomb.

2.10.1. Non-Cellular Honeycomb Modelling

Aktay, Johnson and Kröplin [1] developed a finite element analysis based method of simulating core damage using a semi-adaptive coupling technique. They initially modelled the core as a homogenous solid, simulating damage in the core by replacing any elements whose compressive strain exceeds a predetermined threshold with a cloud of Smooth Particle Hydrodynamics (SPH) particles. This eliminates the sharp drop off of load carrying capacity which would otherwise be seen in a model reliant on element erosion to simulate damage. The experimentation and simulation was conducted to simulate a Nomex™ honeycomb, but the approach should be applicable to aluminum honeycombs as well.

This method can be used to provide a computational simulation of the load versus displacement behaviour of the honeycomb core, which can therefore be used to accurately model the forces upon the face sheets and impactor during an impact event, resulting in accurate estimation of the residual dent profile. The actual damage state of the honeycomb core during and after the impact event cannot therefore be determined, as the actual damage mechanism does not resemble that of the crushing of a honeycomb core. Figure 2-7 show a comparison between the crushing pattern of a Nomex™ honeycomb core and the visualization of the simulation of crushing this core using this process.

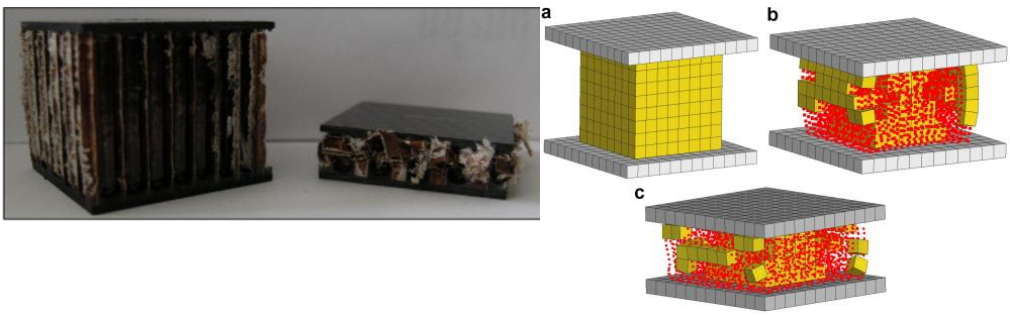

Figure 2-7: Comparison of damage state of crushed Nomex™ honeycomb core (left) and visualization of simulation of crushing process using semi-adaptive coupling technique (right) [1]

Fan, Wang and Sun [42] outlined a method of modelling the honeycomb structure as a homogenous orthotropic solid, with a progressive failure model, which involves modifying (degrading) the stiffness of any element to which sufficient load has been applied to cause yielding. It showed similar results to experimental data, as evaluated by a comparison of the force / distance graphs for the impactor, as well as the damage to the face sheet. Damage to the honeycomb core was not evaluated.

Horrigan and Aitken [40] conducted FEA simulations of impact tests, using an axisymmetric model, which simulated the honeycomb core as a homogenous material with orthotropic stiffness and a continuum damage model criteria. This allows for significantly faster run-times, due to the simplified geometrical representation of the panel and impactor.

2.10.2. Cellular Honeycomb Modelling

Zhang *et al.* [19] conducted a series of simulations and corresponding experiments as validation, modelling the full structure of the honeycomb core, the face sheets and the adhesive layer, without making any significant simplifications for the purposes of cutting down run time. A comparison was made between different material plasticity models. Fully elastoplastic behaviour was shown to be less accurate than bilinear isotropic hardening or a Ramberg-Osgood model [43]. The difference between the bilinear isotropic model and the Ramberg-Osgood model was deemed to be negligible. The effect of omitting or including the adhesive layer in a model

was evaluated. The adhesive layer acted as an additional energy absorber, increasing the amount of kinetic energy absorbed by the panel during the impact by an average of 6.0% across the three simulations which were considered. Overall energy absorption in either case was dominated by the honeycomb core. The honeycomb core in all cases absorbed at least 61% of the total energy absorbed during the impact event. Of that portion, 97% went into causing plastic deformation, as the structure deformed while crushing, with the remained being residual elastic strain energy.

Foo, Seah and Chai [20] conducted similar simulations of impact events by modelling the full honeycomb and panel structure, using a fine mesh in the area immediately beneath the impact. Damage to the honeycomb core was evaluated using plastic strain as the damage criteria.

Nguyen *et al.* [44] conducted a set of simulations for an aluminum – aluminum honeycomb sandwich panel, modelling the 3D structure of the panel including honeycomb with shell elements. The load over time of the impact, the displacement over time of the impactor and the residual dent shape agreed well with their experimental data. They did specify that the model did not represent the core crushing behavior well, as the mesh was not fine enough to properly represent local deformation of the cell walls. Their focus was the evaluation of a program aimed at automatically generating honeycomb structures and other structures such as folded core configurations sometimes used as core material.

Ashab *et al.* [41] conducted their study on the effect of strain rate using FEA. They modelled flat-wise compaction of an aluminum honeycomb core using dynamic FEA with shell elements, a bilinear kinematic hardening material model and a maximum-strain based material failure criterion. Energy dissipation levels and compressive plateau stress were used to evaluate the influence of strain rate on the crushing and indentation processes.

2.11. Residual Strength

In order to determine the residual strength of a sandwich panel following impact, the damage state of the face sheet and core must be accurately determined either through test or simulation. While this thesis did not

consider residual strength, predictions of the damage state will form the starting point for follow-on simulations that will consider measures of residual strength due to different load cases such as bending, compression and tension.

The most common method of determining the effect of impact damage upon the residual strength of a honeycomb sandwich panel found in the literature is through the use of a compression after impact (CAI) test, wherein the impacted panel is subjected to an increasing compressive load, until the onset of failure. The maximum compressive load that the impacted panel can withstand before failure is considered to be the residual strength. The most common failure mode for CAI tests is localized wrinkling of the face sheet leading to buckling [45] and the critical force required to initiate failure has been shown to be a function of the core damage area and depth [46]. This highlights the importance of accurately determining the depth to which damage in the honeycomb core extends. CAI testing also has the advantage of being particularly sensitive to delamination damage [47]; however, this is not a concern for honeycomb panels made with aluminum face sheets.

Even when conducting studies on identical panels, determining trends experimentally can be problematic. There is a significant amount of variation in the measured peak load for CAI for undented panels. Gilioli *et al.* [16] saw this in their extensive testing on aluminum-skinned honeycomb cores. This raises the possibility of minor manufacturer's defects, material imperfections, or other flaws that are not easily detectable playing a large role in the strength of aircraft components.

Three or four point bending tests are also used as a method for measuring the effect of impact damage [17, 45, 46]. In some respects, bending testing may be considered to be more useful, as honeycomb panels in aerospace applications are more often meant to carry a flexural load than a compressive load. However, in these tests failure often occurs prematurely at the supports, making it difficult to determine failure loads for the dented region.

2.12. Topics Requiring Further Investigation

Most work has been conducted on sandwich panels constructed with laminate face sheets and Nomex™ honeycomb cores. The introduction of advanced FEA software packages capable of conducting simulations of impact damage of sandwich panels coincided with a time frame where the aerospace industry was increasingly shifting away from the use of aluminum in favour of lighter panels made out of composite materials. As a result, researchers had a natural tendency to focus their efforts upon the determining the behavior of these newer materials. Due to the different damage modes that occur in aluminum, it would not be reasonable to assume without further investigation that results obtained via testing of laminate / Nomex™ panels are applicable to aluminum panels. The literature is quite sparse when it comes to the investigation of impact damage on sandwich panels of both aluminum face sheets with an aluminum honeycomb core, which will be the focus of this thesis. Metallic panels are still used extensively in legacy aircraft fleets and investigation into their properties is required in order to extend their life-cycles, reduce on-going maintenance costs and ensure safe operations of aging aircraft.

The literature is heavily focused upon research involving spherical impactors and indenters, directly striking the panel perpendicular to its face. As many of the dents which occur in service are caused by impacts with non-spherical objects at an angle to the face sheet, more focus on such impacts would be suitable. Further research on non-standard panels is also warranted, such as the effect of cell wall partition angle on impact damage (beyond the work of Jeon & Shin [21]), the influence of panel curvature and tests on full-size panels rather than coupons.

No comprehensive study investigating the effects of impactor and panel parameters on impact damage in both the face sheet and core was found. Studies which have examined the effects of impactor radius, face sheet thickness, core density and impactor stiffness on the damage in the panel tend to only use two instances of each parameter, which in not sufficient to quantify the relationship. Also, such studies often do not focus on the size and shape of surface dents and very rarely investigate the size and shape of the regions of honeycomb core damage. This thesis aims to address this

gap by using finite element simulations to quantify the effects of face sheet thickness, core density, impactor velocity, mass, stiffness and radius on damage to both the face sheet and the core. The intention is to determine what type of damage is expected so that appropriate representations of the damage state can be used for future work on predictions of residual strength.

3. Methodology

3.1. Introduction

A series of simulations were conducted in order to model the damage created in a honeycomb panel during an impact event. The simulations employed a wide range of different types of impacts and panels to predict the damage caused to both the face sheets and the honeycomb core during impacts and allowed for correlations to be drawn between damage to the panel and the properties of the panel and impactor. The model simulates a spherical object being dropped onto a section of panel with a specified initial impact velocity. The individual cells of the honeycomb core were modelled in order to accurately capture the buckling and crushing behavior. Figure 3-1 shows a view of the panel and impactor modelled.

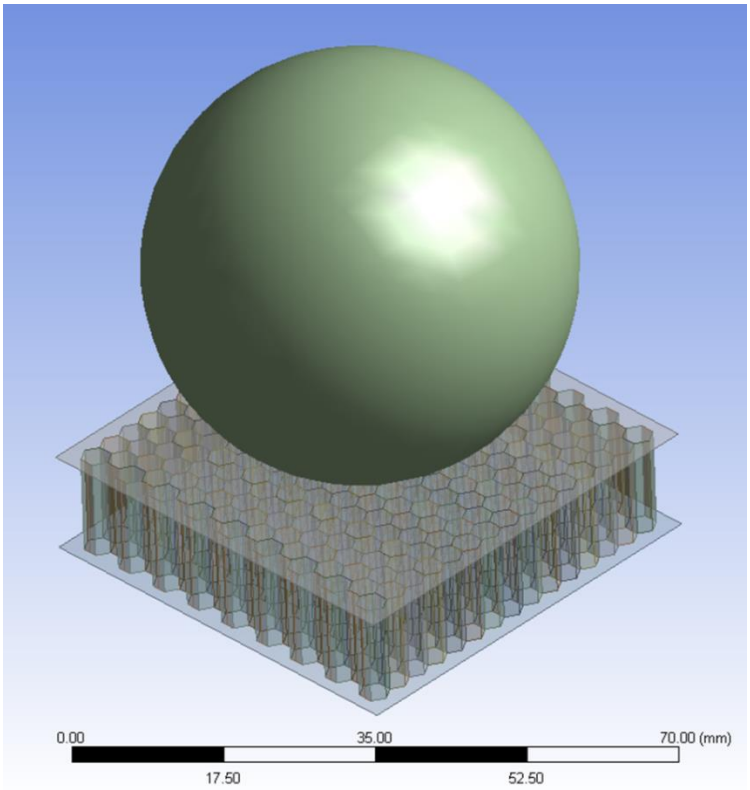

Figure 3-1: Geometry of honeycomb sandwich panel section and impactor

The general purpose finite element analysis package ANSYS was used for all simulations. It is a software package widely used in industry and academia in order to conduct simulations on structures, fluids and electrical applications. The Explicit Dynamics subset solver package of the application is well suited for modelling short-duration impact events between objects. The effects of the objects mass, inertia and momentum, appropriate constraints and boundary conditions, contact between objects, stress wave prorogation, elastic deformation, material plasticity and material failure criteria are all accounted for. This enables the progressive crushing of the honeycomb core to be simulated.

3.2. Baseline Model

A model of a section of a honeycomb panel was built to be used as an initial baseline. Subsequent studies were conducted by varying the following parameters of the baseline model: impactor mass, impact velocity, impactor radius, impactor stiffness, face sheet thickness, core cell wall thickness, core cell size and panel thickness. The specifications of the initial model were based upon a sample panel used aboard the Bell CH-146 Griffon series of tactical helicopters, currently in use by the Royal Canadian Air Force in Search and Rescue and Tactical Airpower Support roles.

The panel for the baseline model consists of two 0.301 mm (0.012″) thick aluminum face sheets separated by a 12.7 mm (0.5″) thick section of aluminum honeycomb core. The honeycomb core is a hexagonal lattice structure, with cells 3.175 mm across (1/8th″), flat to flat. The cell walls in the ribbon direction, L, are 0.0508 mm (0.002″) thick, while the off-ribbon cell walls are 0.0254 mm (0.001″) thick. Figure 3-2 shows a diagram of a single cell of the honeycomb core and the overall structure of the honeycomb once extruded and mirrored.

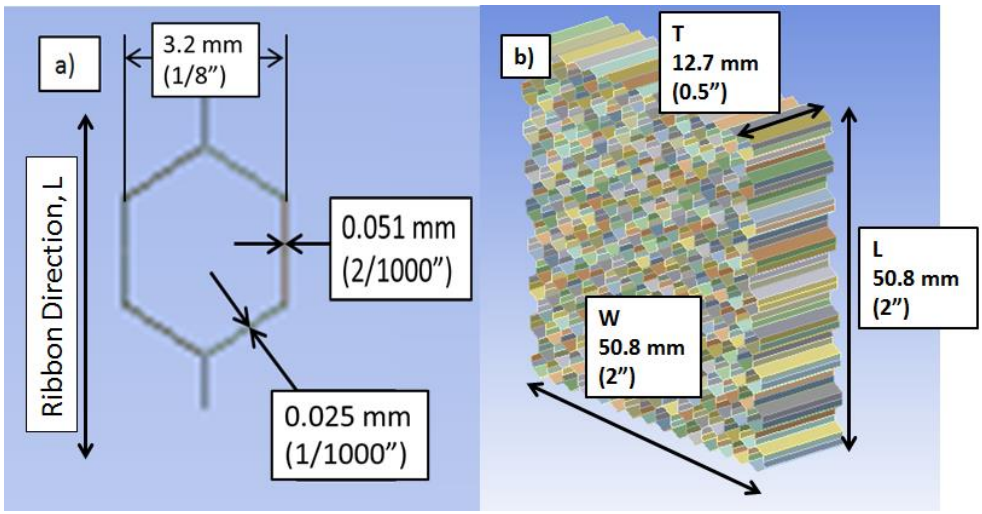

Figure 3-2: Diagram of the honeycomb core, showing; a) single cell and b) overall lattice

3.3. Baseline Geometry

A 50.8 mm x 50.8 mm (2″ x 2″) section of this panel is used for all models. This size was chosen to be large enough to capture the entirety of the damage caused during the impact events.

DesignModeler, the solid modeler built into ANSYS Workbench, was used to construct the geometry of the sandwich panel. Surface bodies were used for the construction of both the face sheet and the cell walls of the honeycomb core, to allow for the use of shell elements in the mesh. This is similar to the approach taken by Zhang *et al.* [19], Foo, Seah and Chai [20], Ashab *et al.* [41] and Nguyen *et al.* [44]. The use of planar elements instead of solid elements is especially important in explicit dynamic FEA for objects such as the cell walls of the honeycomb core or the aluminum face sheets, whose thickness is much smaller than their length and width. Solid elements may be able to provide more detailed solutions in terms of through-thickness deformation, which would require bodies with at least two elements through the thickness, resulting in elements with one very small dimension. The maximum time step used during an explicit analysis is proportional to the size of the smallest dimension in any element. This ensures that the pressure wave does not skip any elements during any iteration. The small through-thickness element dimensions required for a solid element model would lead to unmanageable run times, hence the choice of planar elements.

A section of the honeycomb core was constructed, consisting of one off-ribbon direction cell wall and two half-walls in the ribbon direction, with appropriate surface body thicknesses assigned. This unit cell, shown in Figure 3-2, was then mirrored as needed in order to create a suitably large section of the honeycomb core.

Another pair of surface bodies was added, to form the top and bottom face sheets, with the 0.301 mm surface body thicknesses assigned. Sections of the honeycomb core which extend beyond the edges of the face sheets were then suppressed. Finally, a solid sphere 25.4 mm (1″) in diameter was created, positioned above the middle of the top face sheet, with a gap of 0.0254 mm (0.001″) between the face sheet and the surface of the sphere.

This gap is small enough that, with the initial impactor velocity prescribed, the contact between impactor and face sheet occurs 12.7 μs after the simulation has started.

3.4. Baseline Material Models

The face sheets are 7075-T6 aluminum, the honeycomb core is 5056-H38 aluminum and the spherical impactor is structural steel, with material properties as outlined in Table 3-1**Error! Reference source not found.**. The impactor is modelled using a linear elastic material model, as the impactor is not expected to yield given the relative stiffness of the two components, while plasticity within the face sheets and honeycomb core are modelled using bilinear stress-strain curves. Element erosion is used to model the failure at the maximum equivalent plastic strain within an element.

Table 3-1: Material properties for FEA simulation

	7075-T6 (Face Sheet)	5056-H38 (Core)	Structural Steel (Impactor)
Density (kg/m$^{3)}$	2804	2640	7850
Young's Modulus (GPa)	71.7	71	200
Poisson's Ratio	0.33	0.33	0.30
Yield Strength (MPa)	503	345	N/A
Tangent Modulus (MPa)	500	500	N/A
Max. Equivalent Plastic Strain at Failure	0.11	0.15	N/A

In terms of material plasticity and eventual failure of the aluminum components, the material model will be conservative, as the damage created in the panel simulation will be more extensive than would be expected in an actual simulation. Figure 3-3 shows a comparison between the assumed bilinear stress strain behaviour for the material model of the 7075-T6 aluminum and published experimental data [48].

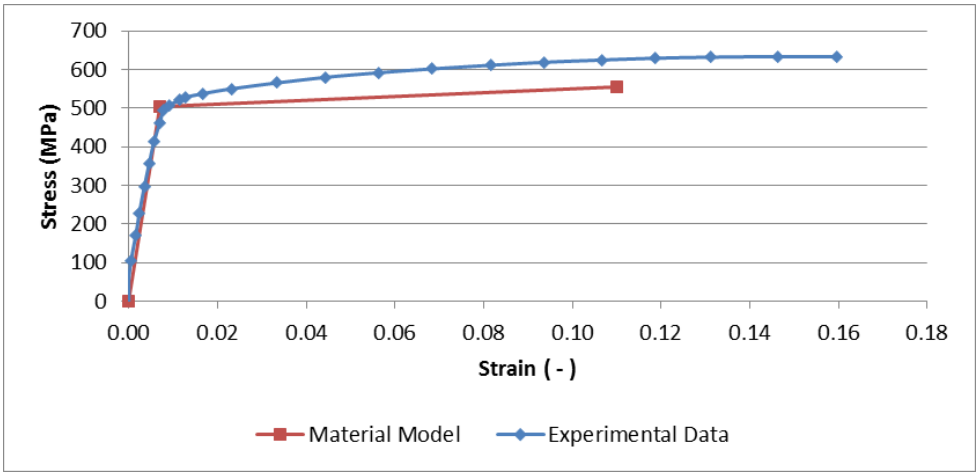

Figure 3-3: Stress - strain comparison of bilinear material model for 7075-T6 aluminum and experimental data [Adapted from Reference 48]

3.5. Element Meshing

In order to ensure a higher degree of accuracy while minimizing simulation run-time, a finer mesh was used in an inner core region of 23 cells in the centre of the honeycomb core, in the area near the impact and a coarser mesh is used outside that region. Figure 3-4 shows a cross section view of the resultant baseline model and its mesh. The model as a whole had 19145 nodes and 25520 elements. This inner core region is highlighted in Figure 3-5. This allowed the model to capture the more extreme deformations and stresses occurring closest to the impact more accurately.

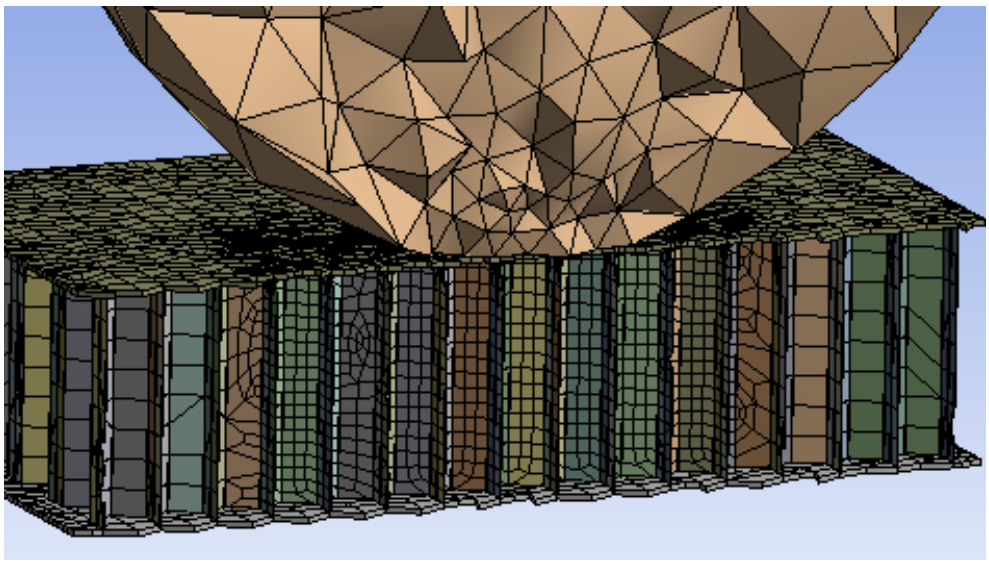

Figure 3-4: Cross section view of meshed baseline model

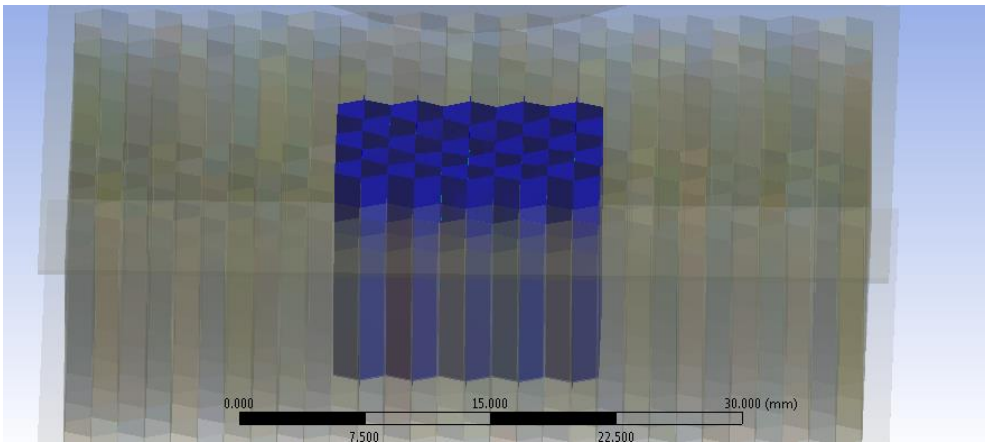

Figure 3-5: Inner core region for finer mesh size setting

A sphere of influence style mesh sizing was used to create a finer mesh in the spherical impactor at the point of impact, while having a very coarse mesh outside that area. As the stresses in the impactor are not of interest, a fine mesh is only needed in the contact region. No mesh sizing parameters were set for the face sheets, allowing the density and distribution of the mesh in those bodies to be driven by the settings for the honeycomb core. Lower order elements were used because the Explicit Dynamics solver does not support higher order elements. Shell elements with 6 degrees of freedom were used for the face sheets and the honeycomb core cell walls, which allowed for the elements in those structures to carry axial, bending, shear, and torsional loads.

This mesh sizing was obtained after an initial mesh convergence study was conducted. Figure 3-6 shows the resultant dent depth and simulation run time for the mesh sizes considered. The sizing of 3 elements across the off-ribbon directions and 4 elements across the ribbon direction provided an appropriate trade-off for accuracy versus run time; using a finer mesh than this resulted in drastically longer run times, with only minor increases in accuracy. All simulations were conducted using a computer system with a deca-core 2.30 GHz processor with 18 GB of Random Access Memory (RAM).

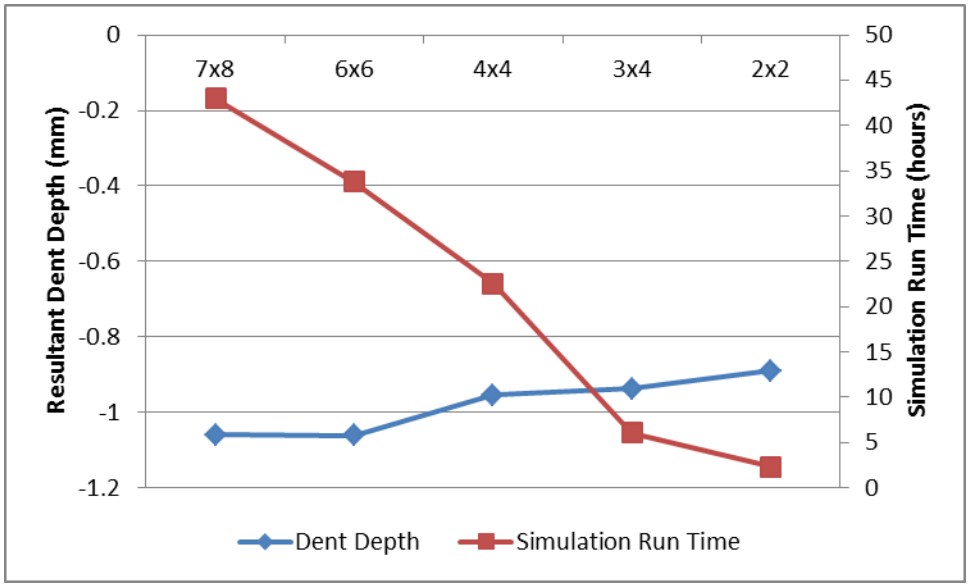

Figure 3-6: Resultant dent depth and simulation run time variation for different mesh sizes

3.6. Constraints and Initial Conditions

The bottom face sheet of the honeycomb panel was fixed in all degrees of freedom, preventing any rotation or displacement. This would be equivalent to a coupon-level test wherein the bottom face sheet had been adhered to a rigid platform prior to impact. An impact simulating a section of an in-service panel would be better represented by a constraint on the edges. Some very high energy impacts can cause yielding on both the front and back faces of the panel. However this would not occur with the low-velocity impacts that are the focus of this thesis. In such cases, the question of whether or not the damaged panel will require replacement or repair is undoubtedly in the affirmative. In the lower energy impacts under consideration in this thesis, that effect will not occur, thus fully fixing the bottom face sheet is not likely significantly decrease the accuracy of the results obtained. The effect that imposition of boundary conditions on the edges of the panel can have on the results obtained are discussed in more detail in Section 5.2.2.

The impactor was placed 0.0254 mm (0.01") from the surface of the top face sheet, above the centre of the face sheet (which is also in line with the centre of one of the honeycomb cells) and given an initial velocity, causing a perpendicular impact against the face sheet. The initial velocity for the baseline model was 2 m/s. This velocity was chosen in order to produce a residual dent within the allowable dent limits for similar panels used on the Griffon helicopter. The effect of gravity was not considered, as its overall effect would be minimal given the short duration of the impact simulation.

3.7. Analysis Settings

In order to ensure that the impact event was simulated until completed, the simulation run time was set to 3 ms. The minimum and maximum time step setting was kept as "Program Controlled", which allowed the software to adjust the time step needed, based upon strain simulated during the modelling. The time step safety factor setting was set to 0.9 which ensured that the minimum time step was low enough that the shock wave associated with any force applied during the simulation, travelling through the object at the speed of sound for that material, could not propagate any through the material fast enough that it would completely skip past any single element during a time step. Thus the minimum time step is a function of the speed of sound through the material and the mesh sizing, being proportional to the smallest distance between two nodes in the structure. Higher speeds of sound or coarser mesh sizing therefore both correspond to a faster simulation run time. Automatic mass scaling, a technique which artificially increased the mass of components in the model due to the effect that density has upon the speed of sound through an object, which can therefore increase the minimum time step, was not used.

Contact was defined between all surfaces within the model as being frictionless, which captured the interaction between the impactor and the face sheet, as well as between the face sheet and cell walls and between adjacent cell walls as they collapsed. This utilizes the penalty method of contact modelling. The tangential components of any contact force are expected to be negligible, therefore using a frictionless contact model is appropriate.

3.8. Variations to Baseline Simulation

Seven different studies were conducted, that varied different properties of the impact and the panel. The purpose was to generate a wide range of different types of damage so that relationships between damage and the input parameters could be determined. For each series, parameters of the baseline model were altered as outlined in Table 3-2. The range of values was chosen in order to create damage within the VID range, both within and above the negligible damage limits [33]. The seven studies considered impactor velocity, impactor mass (the velocity and mass were chosen to produce the same kinetic energy), impactor size (adjusting the density in order to maintain a constant mass and kinetic energy level), impactor stiffness, face sheet thickness, honeycomb core density (adjusting the cell wall thickness and the cell size) and sandwich panel thickness. The mesh sizing remained the same across all simulations, with the exception of the core density study. Because of the changing cell size, this study used a constant element size of 1.2 mm for the honeycomb core, instead of a constant number of elements across each cell wall. Figure 3-7 shows a comparison of the meshes for the largest and smallest cell sizes, respectively. The mesh sizing for the impactor and all other parameters were kept the same as the baseline model. The parameters were varied independently, so any interaction between them is not considered.

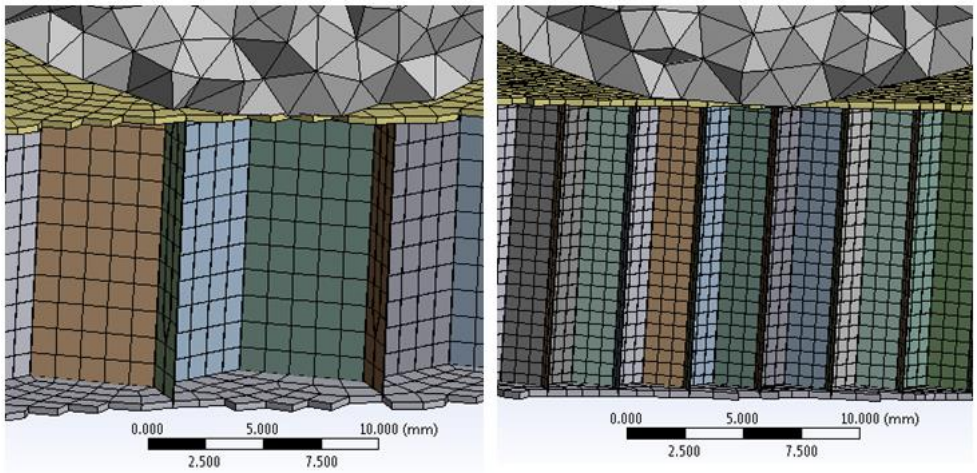

Figure 3-7: Comparison of meshes for panels with cell sizes of 9.5 mm and 3.2 mm, from core density study

Table 3-2: Parameters varied for each series of simulations, with bold entries indicating the parameters of the baseline model.

Parameter / Study	Impactor velocity (m/s)	Impactor Mass (kg)	Impactor Radius (mm)	Impactor stiffness (GPa)	Face Sheet Thickness (mm)	Core cell wall thickness (mm)	Core cell size (mm)	Panel thickness (mm)
Impactor Velocity	1.5, **2.0**, 2.5, 3.0, 3.5, 4.0	0.54	25.4	200	0.30	0.025	3.2	12.7
Impactor Mass	2.0	0.30, **0.54**, 0.84, 1.21, 1.64, 2.15	25.4	200	0.30	0.025	3.2	12.7
Impactor Size	2.0	0.54	6.4, 12.7, 19.1, **25.4**, 31.8, 38.1, 50.1	200	0.30	0.025	3.2	12.7
Impactor Stiffness	2.0	0.54	25.4	0.1, 1, 10, 50, **200**, 400	0.30	0.025	3.2	12.7
F7ace Sheet Thickness	2.0	0.54	25.4	200	0.10, 0.15, **0.30**, 0.46, 0.61, 0.91, 1.22	0.025	3.2	12.7
Core Density	2.0	0.54	25.4	200	0.30	0.018, **0.025**, 0.051	**3.2**, 4.8, 6.4, 9.5	12.7
Panel Thickness	1.5, **2.0**, 2.5, 3.0, 3.5, 4.0	0.54	25.4	200	0.30	0.025	3.2	**12.7**, 8.89, 5.08, 2.54

3.9. Extraction of Damage Results

The simulations covered the time from the start of the impact until after the impactor had rebounded and sufficient time had elapsed to allow for any elastic spring back of the face sheet and core to occur. For the baseline model, this impact event simulation represented 2.1 ms in real time, although some following simulations conducted required up to 3.6 ms. A residual dent is identified as the section of the face sheet that has any downward deformation greater than 0.01 mm after the elastic spring back. This threshold was chosen because it is the value at which all simulations demonstrated the most pronounced transition between a relatively flat profile and a distinct dent shape. The dent depth is the maximum downward post spring-back deflection of the face sheet from its original position. The dent width is the distance between the two points along the dent profile where the 0.01 mm threshold is crossed. Figure 3-8 shows an example dent profile with the dent width and dent depth measurements noted.

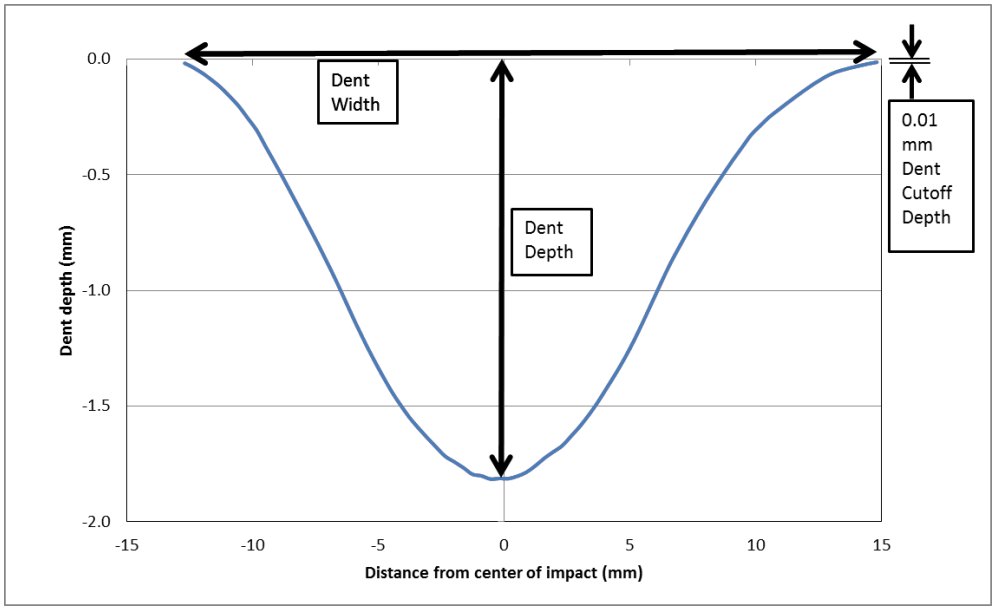

Figure 3-8: Dent width and depth measurements for representative dent profile

The honeycomb core damage was measured by examining a cross section view of the core across the diameter of the dent. All sections of the core which had experienced plastic strain above the 0.2% limit typically used to define the onset of yielding are considered to be damaged, similar to the approach taken by Foo, Seah and Chai [20]. Both the maximum and average depths of the core damage were measured. The maximum depth is the maximum depth to which the yielding extended over the entire damage region. The average depth was determined by taking the maximum depth to which this yielding extended per cell wall and averaging it across the entire width of the damage area. The width of the damage zone was taken as the width across all cell walls which experienced yielding (in full-cell increments). Figure 3-9 shows an example of such a measurement.

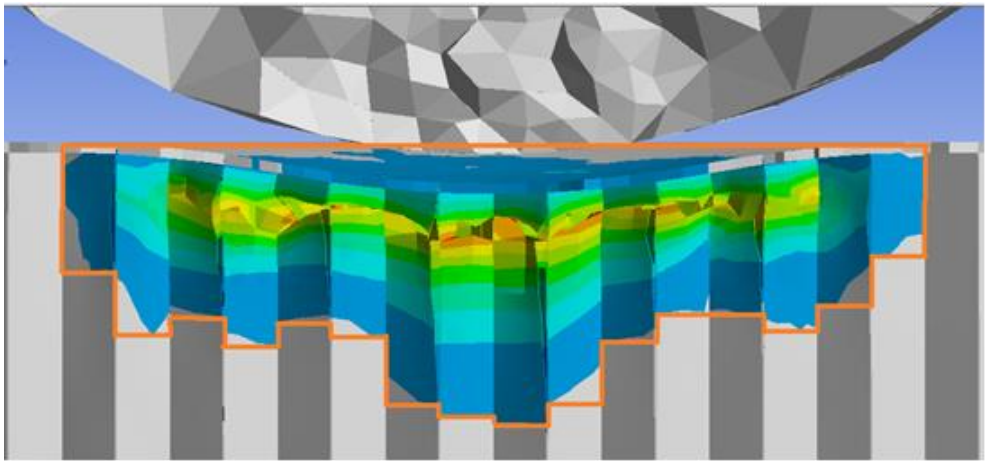

Figure 3-9: Core damage measurement with coloured region indicating yielding (light blue being the onset of yielding and red indicating the highest levels of plastic strain) and the entire damage region in increments of full cells outlined in orange

4. Results

4.1. Typical Impact Damage Progression

Impacts to metallic honeycomb sandwich panels cause two forms of damage. The more obvious damage is the denting of the face sheet that is impacted. This results in a measurable residual surface depression which depending on the magnitude of the depth and width, may or may not be considered easily visible. The second type of damage caused is to the core, which experiences crushing underneath the surface of the dent and depending upon nature of the impact, may also experience cracking or splitting of the cell walls, or segments thereof. A typical impact event progresses in 5 different stages, as illustrated in Figure 4-1:

- The initial impact causes bending of the face sheet, resulting in the initial downward deflection at the point of impact. The section of the core underneath the impact area immediately experiences yielding and some lateral displacement.

- Buckling occurs in the core cell walls beneath the impact. The cell walls in the damage region begin crushing as the cell walls fold in upon themselves.

- The damage region in the honeycomb core spreads widthwise as the face sheet dent widens and deepens. The honeycomb core damage region remains the same depth.

- The maximum dent depth is reached. The extent of the damage region of the honeycomb core is determined at this point.

- Elastic spring back of the face sheet occurs as the impactor rebounds. The face sheet settles into the shape of the residual dent profile as the impactor loses contact with the face sheet. The honeycomb core, having absorbed energy resulting in plastic deformation as part of the crushing process, goes into tension as the face sheet dent relaxes.

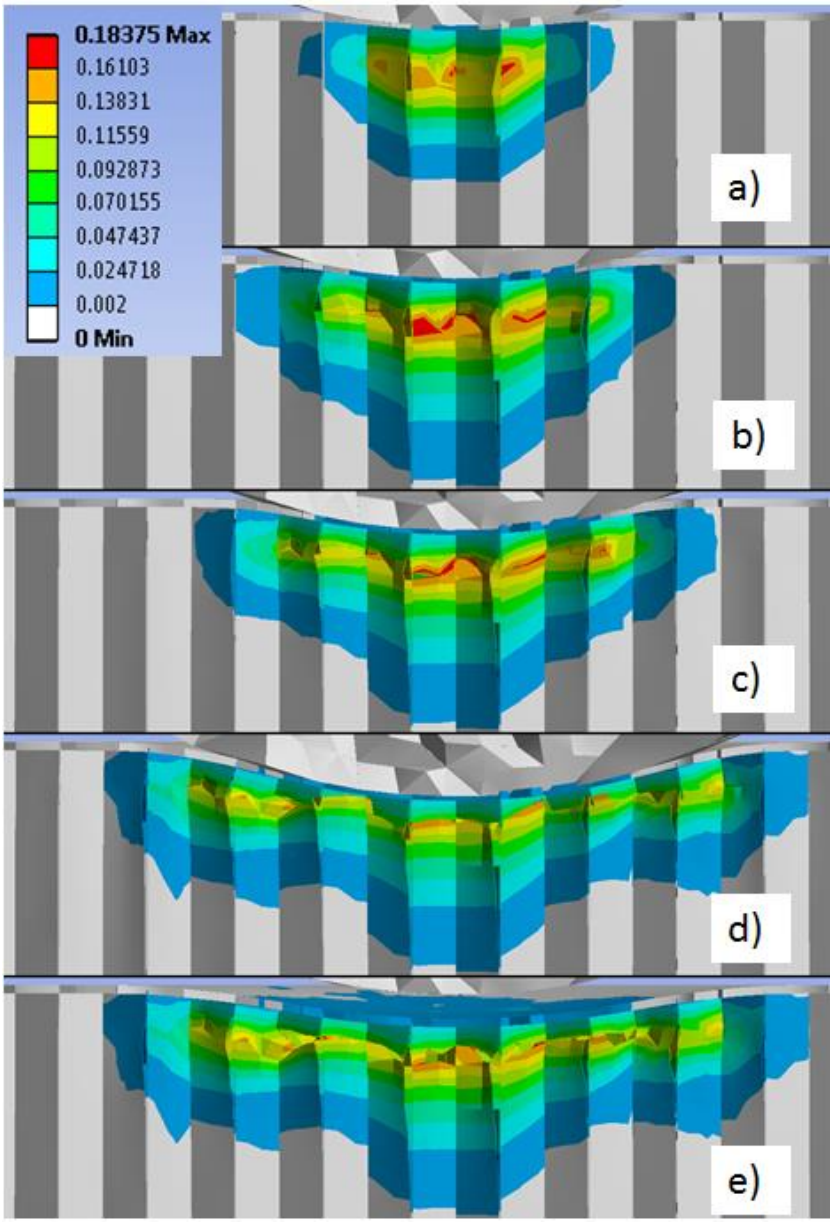

Figure 4-1: Typical progression of an impact event with the coloured region indicating plastic strain (contour at top left is valid for all stages of impact): a) initial damage immediately after impact, b) crumpling begins, c) damage region spreads outwards as dent deepens, d) dent reaches maximum depth and e) face sheet relaxes to residual dent shape

Figure 4-2 highlights the residual tensile stress in the honeycomb core following spring back, largely localized beneath the dent, with the coloured areas showing tensile normal stress in the out-of-plane direction.

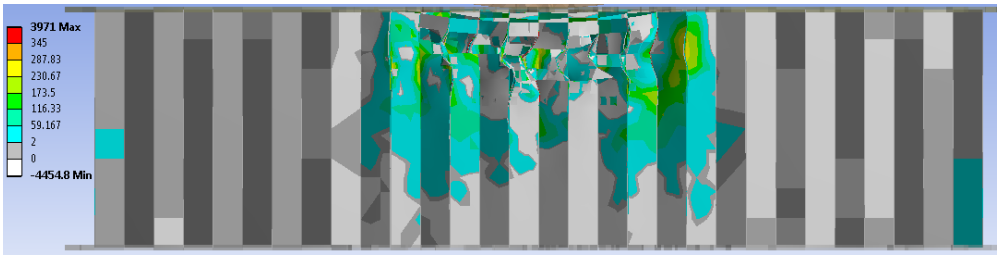

Figure 4-2: Distribution of normal tensile stress in out-of-plane direction (MPa), post-impact

4.2. Damage to the Face Sheet

Damage to the face sheet was measured in terms of dent depth and width. Dents ranged from 0.51 mm to 2.42 mm deep and 14.3 mm to 43.6 mm wide. The limit at which a dent is deemed to be negligible in the Griffon SRM for panels of this size is a width of 12.7 mm, with no depth criteria [33]. In two instances, the impact with the highest impactor mass and the impact with the smallest impactor radius, the face sheet was ruptured, which would mandate repair.

4.2.1. Face Sheet Cracking

Face sheet cracking occurred in two of the simulations conducted: from the size study, the simulation with the smallest radius (6.35 mm) and from the mass study, the simulation with the highest mass (2.2 kg). Figure 4-3 shows a top-down view of the dented area of the face sheet from the 6.35 mm impact, with all the coloured sections indicating areas which have experienced yielding. The hole caused by the impact is magnified.

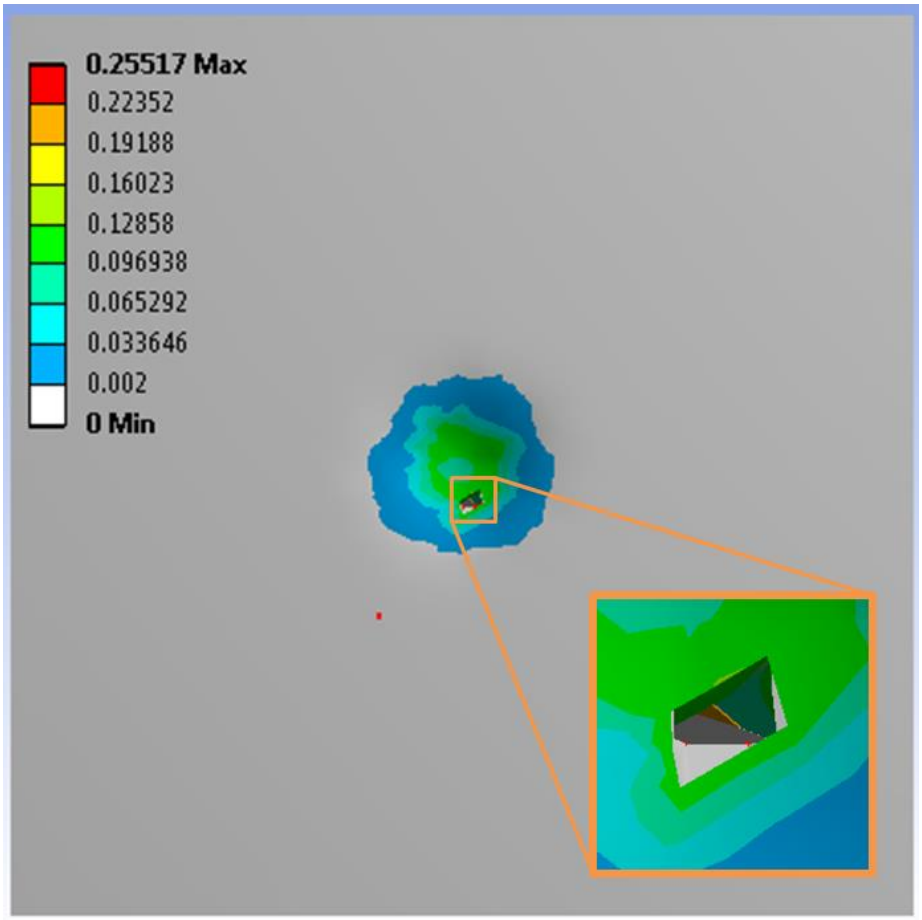

Figure 4-3: View of plastic strain in face sheet, including hole caused by material failure, for 6.35 mm radius impactor

These two simulations both had the highest ratio of impact energy to surface area of the dent, at 1.66 mJ/mm^2 and 1.62 mJ/mm^2, respectively, with the former having a smaller total energy concentrated into a smaller area and the latter having a larger energy spread over a wider area. It is this elevated energy concentration which resulted in the surface rupture.

None of the other simulations conducted resulted in material failure of the face sheet. Each of those had a lower energy concentration of impact energy over the dent area, with the next highest being 1.3 mJ/mm^2.

4.2.2. Kinetic Energy Series

The initial kinetic energy of the impactor was varied between 0.61 and 4.31J for this series of simulations, by varying either the velocity of the impactor, or its mass (accomplished by adjusting the density of the impactor). The velocity was varied from 1.5 to 4 m/s and the mass was varied from 0.323 to 2.16 kg. Twelve simulations were performed for this study, with all other parameters matching the baseline model.

Increasing the kinetic energy of the impactor via either mass or velocity resulted in a linear increase in the residual dent depth as shown in Figure 4-4 and a logarithmic relationship for dent width in Figure 4-5. In order to absorb the impact of the higher kinetic energy levels, the impactor displaced further downwards, which caused a wider section of the face sheet to be pulled downwards, resulting in the deeper and wider dent. Increasing the velocity results in a larger dent depth and dent width than when the mass was increased.

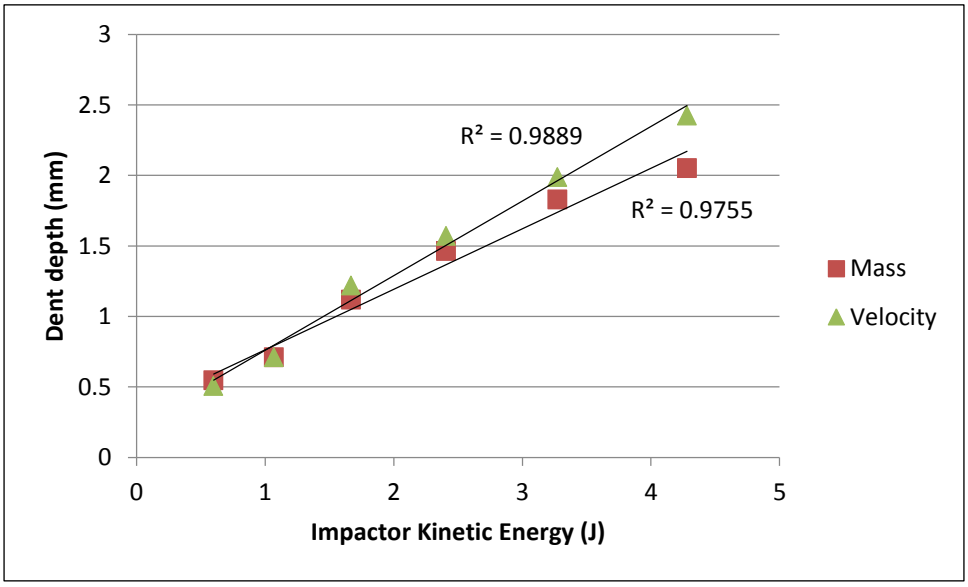

Figure 4-4: Residual dent depth variation with impactor kinetic energy

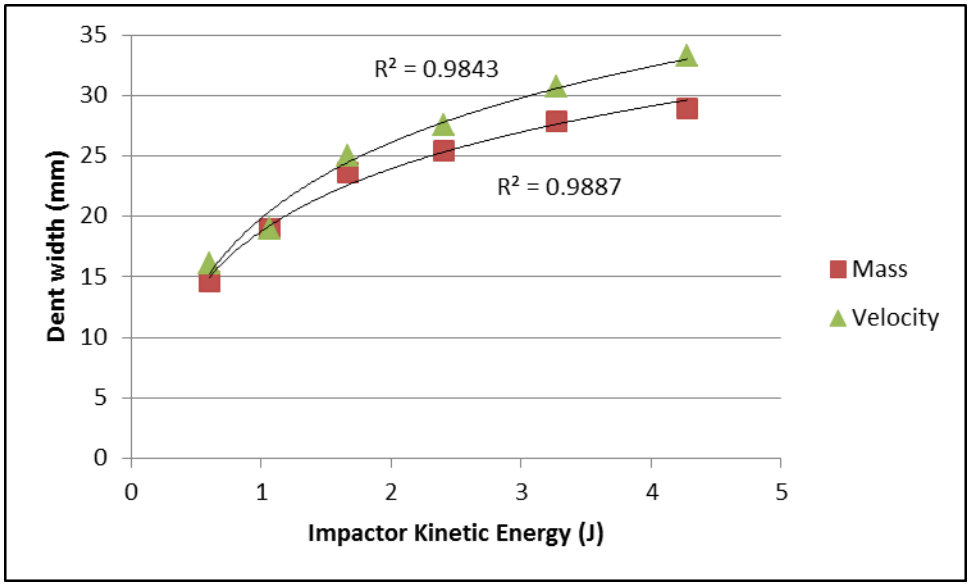

Figure 4-5: Residual dent width variation with impactor kinetic energy

Figure 4-6 presents the resultant dent profiles for the six impact velocities simulated, where the dent depth can be seen to increase more than the dent width. The six simulations varying the mass of the impactor showed the same trend. The relationship between dent depth and width can be seen in Figure 4-7 in terms of the aspect ratio of the dent (width/depth) when either the velocity or mass was changed. Its negative slope indicates that the dent depth increases more than the width as impact energy increases, varying with a 2nd order polynomial relationship.

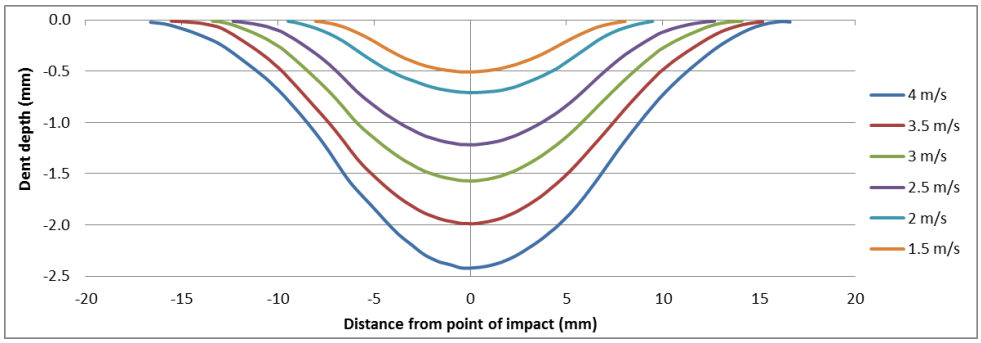

Figure 4-6: Resultant dent profiles for varying impact velocities

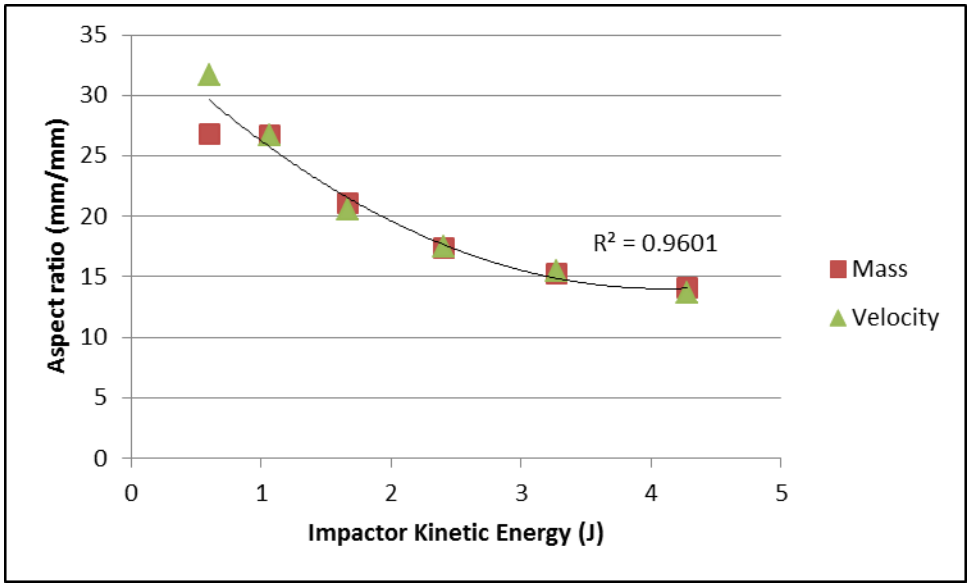

Figure 4-7: Aspect ratio (width / depth) of dents for varying impact kinetic energy levels

4.2.3. Impactor Radius Series

The radius of the impactor was varied between 6.35 and 50.8 mm for this series of seven simulations. In order to ensure that the size was the only factor being changed, the density of the impactor was adjusted in order to maintain a constant mass of 0.538kg and a resulting kinetic energy of 1.07J. All other parameters matched the baseline model.

Increasing the radius of the impactor while maintaining constant impact energy resulted in wider, shallower dents for constant impact energy as seen in Figure 4-8. With a larger impactor, the change in curvature between the undamaged section of the face sheet and the dent becomes less severe. The aspect ratio of the dent (width/depth) increased with increasing impactor radius as illustrated in Figure 4-9, indicating that a larger impactor caused wider, less deep dents, with the aspect ratio varying according to a 2nd order polynomial relationship. Smaller impactors concentrate the impact energy into a smaller section of the face sheet, causing more localized deformation. As a result, the downward deflection does not spread as far radially as the impact energy is absorbed.

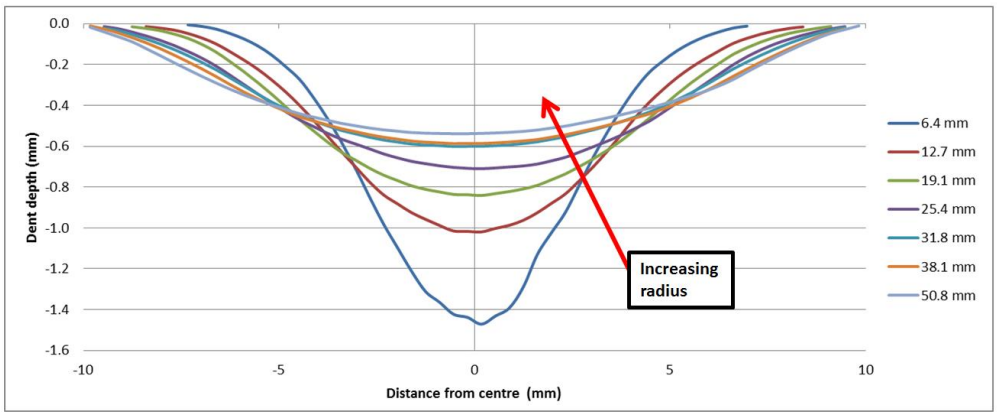

Figure 4-8: Resultant dent profiles for varying impactor radii

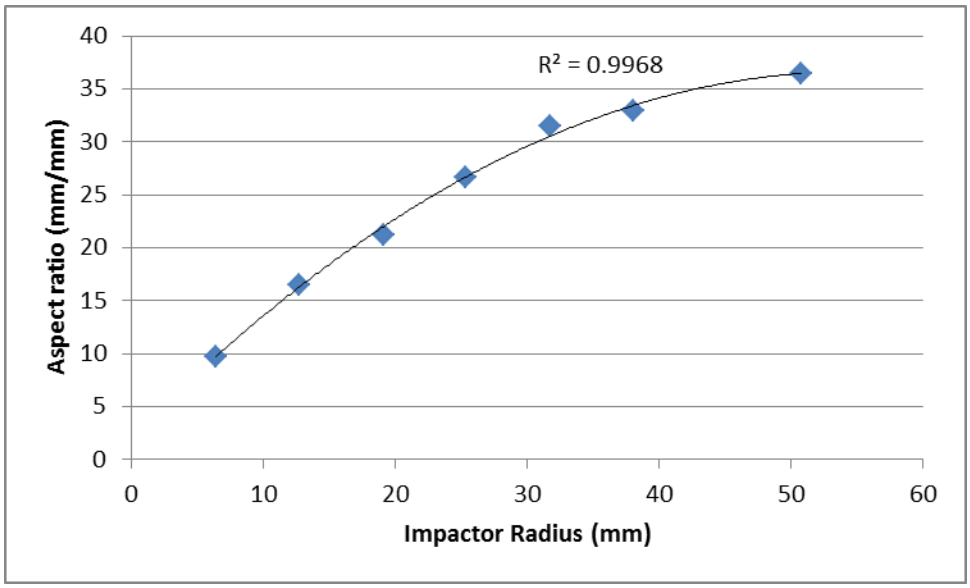

Figure 4-9: Aspect Ratio (width / depth) of dents for varying impactor radii

4.2.4. Impactor Stiffness Series

For this series of six simulations, the Young's modulus of the impactor was varied between 0.1 and 400 GPa. Table 4-1 outlines typical materials [49] that have the Young's moduli used in the study. All other material properties (including density) were kept the same as structural steel and all other parameters were the same as the baseline model.

Table 4-1: Young's Moduli used in simulations and comparative material in same stiffness range

Young's Modulus (GPa)	Comparison Material
400	Tungsten (400 GPa)
200	Stainless Steel 405 (200 GPa)
50	Tin (44.3 GPa), Magnesium (45 GPa)
10	Graphite (11 GPa), Red oak - parallel to grain (11 – 14.1 GPa)
1	Polypropylene (1.14 – 1.55 GPa)
0.1	Low-density polyethylene (0.17 – 0.28 GPa)

As the stiffness of the impactor decreased, the effect on the dent profile was minimal within the range of 10 – 400 GPa. However when the Young's Modulus dropped from 10 to 0.1 GPa the depth and width of the dent decreased by 35 and 19%, respectively. Figure 4-10 shows the variation of the dent depth (left axis) and dent width (right axis), respectively, with stiffness.

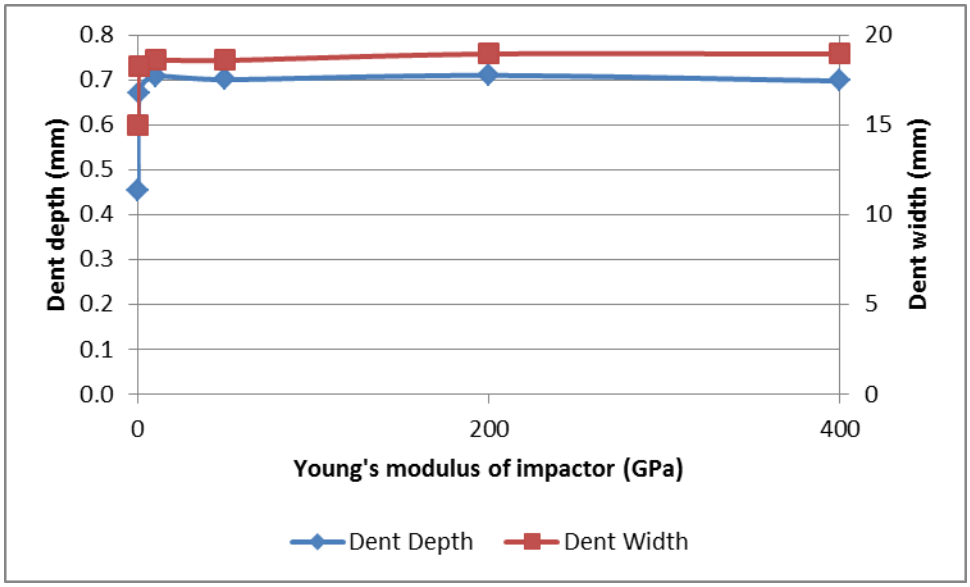

Figure 4-10: Dent depth (left axis) and dent width (right axis) versus Young's Modulus of impactor

The impactors with lower stiffness experienced more elastic deformation during the impacting process, flattening against the top face sheet. Figure 4-11 shows a comparison of the elastic strain in the impactor at the point of maximum deflection for the 0.1 GPa impactor and the 400 GPa impactor, where the least stiff impactor had substantially more elastic deformation. This increased deformation resulted in a larger portion of the total energy being temporarily transformed into elastic strain energy stored within the impactor, until the impactor started to rebound, after which the elastic strain energy was transformed back into kinetic energy, resulting in a higher rebound velocity. Therefore, for the stiffer impactors, a larger portion of the total energy was transferred into the sandwich panel, resulting in more plastic deformation of the face sheet and the honeycomb core. Figure 4-12 outlines the effect that the impactor stiffness had upon the amount of percentage of kinetic energy absorbed by the sandwich panel during the impact event. The kinetic energy absorption was determined by examining the remaining velocity of the impactor, after the impact event. It is expected that when a stiffer object impacts a softer object, the softer object will be the one to be absorbing the bulk of the energy of the impact, whereas objects who have an equivalent Young's modulus would be

deforming equally and energy absorption will be more evenly distributed. The sharp transition observed in impact damage caused when the impactors stiffness drops below 1 GPa is likely when the Young's modulus of the impactor approaches or drops below the equivalent stiffness of the panel as a whole, although that value was not quantified in this study.

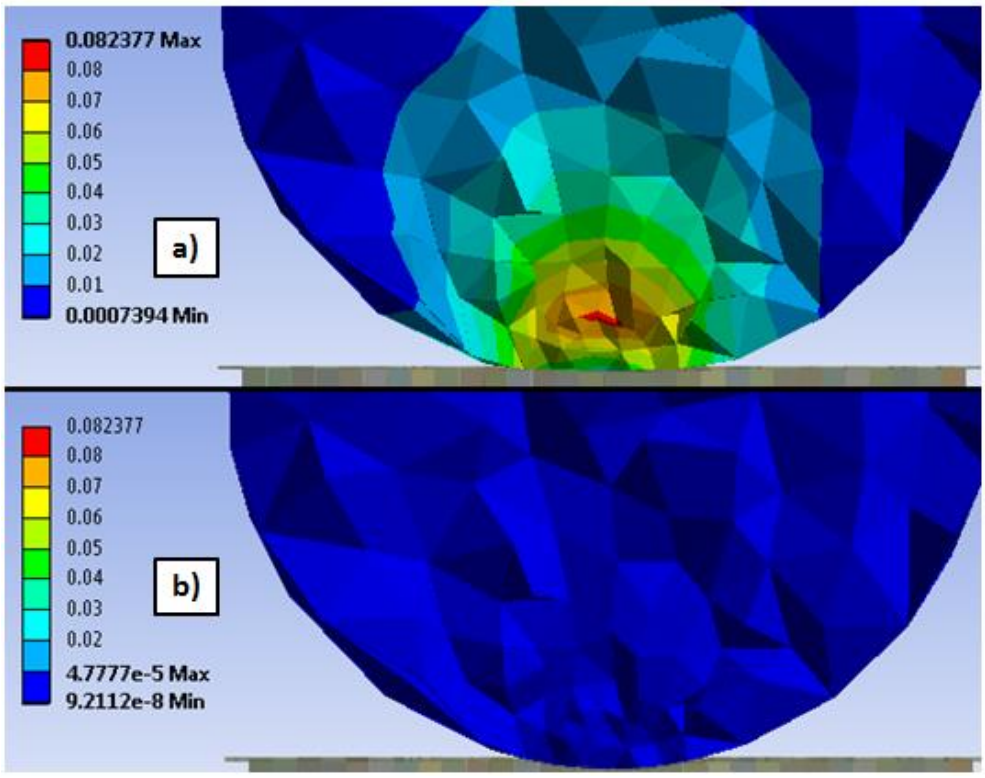

Figure 4-11: Elastic strain in impactor, using same scale, at point of maximum displacement for a) E = 0.1 GPa and b) E = 400 GPa.

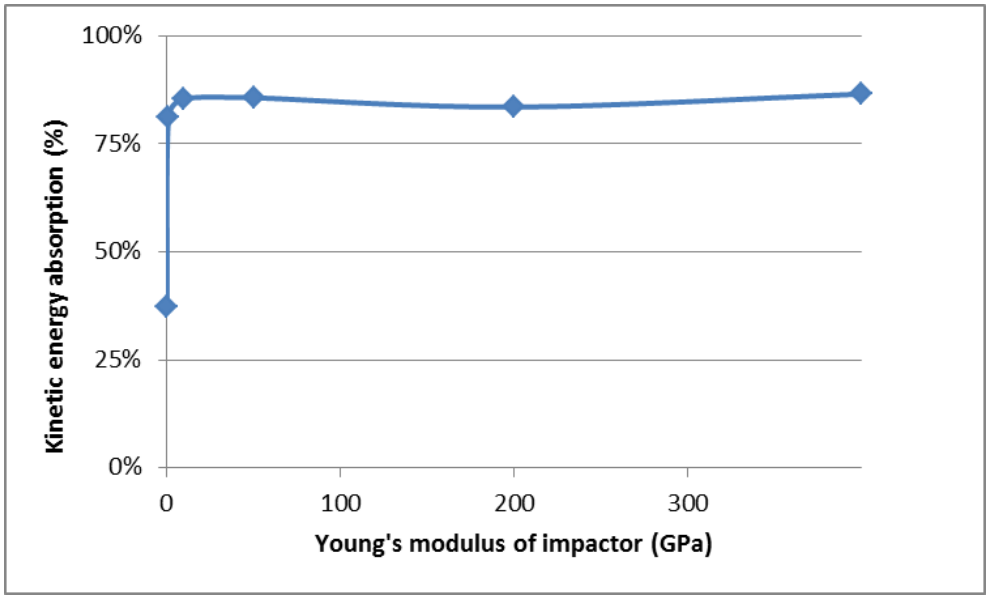

Figure 4-12: Percentage of kinetic energy absorbed by panel during impact, as function of Young's modulus of impactor

4.2.5. Face Sheet Thickness Series

The thickness of the face sheets were varied from 0.102 to 1.219 mm for this series of seven simulations. All other parameters matched the baseline model and the kinetic energy was kept constant.

Thicker face sheets resulted in shallower dents, as shown in Figure 4-13, due to the increased energy absorbed by the face sheet. While the dent depth decreased by 70% as the thickness was increased from 0.102 to 1.219 mm, the dent width only increased by 14%. The smaller effect on dent width occurs because thicker face sheets tend to spread out the surface damage. When the stiffer face sheet deforms, the damage is not contained to a region directly under the impactor, rather the bending in the thicker skin also causes core damage in the region surrounding the impactor. Figure 4-14 shows that the aspect ratio of the dent (width/depth) increases linearly with increasing face sheet thickness, due to the decrease in the dent depth.

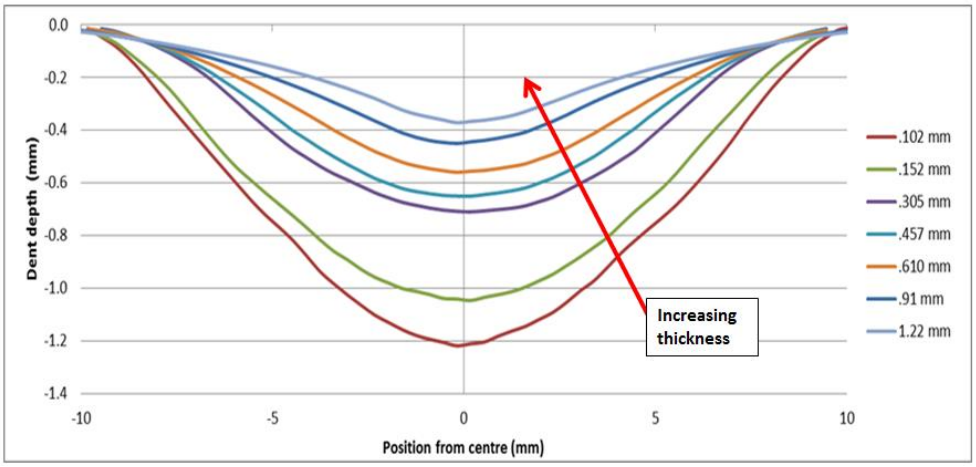

Figure 4-13: Resultant dent profiles for varying face sheet thicknesses

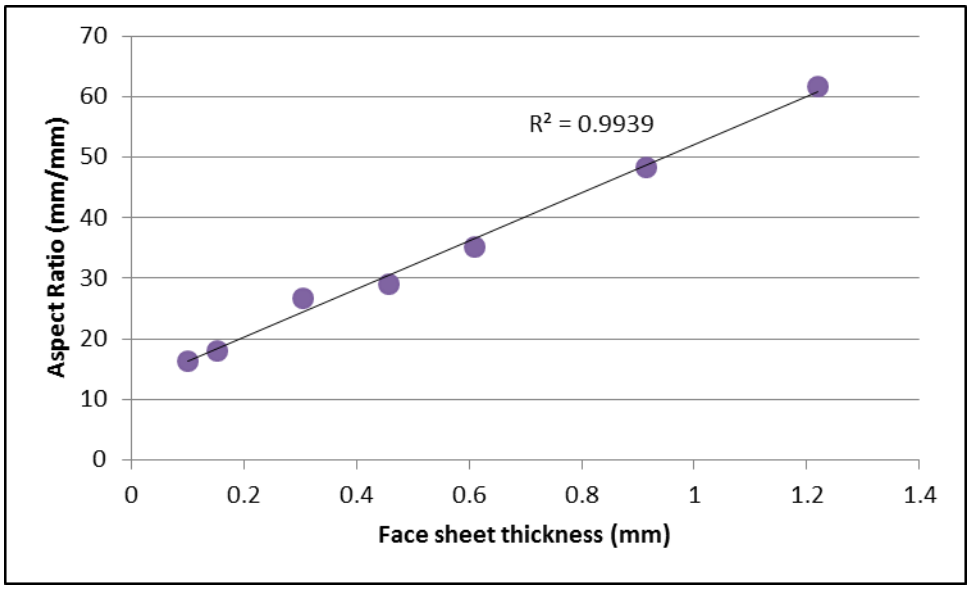

Figure 4-14: Variation of aspect ratio (width / depth) of dent profile versus the face sheet thickness

A thicker face sheet is stiffer and more resistant to bending than a thinner face sheet. This causes a smoother transition between the dent and the undamaged portion of the face. A thicker skin will result in a less deep dent, but the skin itself is also more resistant to bending, resulting in less

curvature both at the bottom of the dent and around the rim of the dent. Figure 4-15 shows a comparison of the damage regions for the impact simulations on the thinnest and thickest face sheets, respectively. While the planar size of the dent is similar, the thinnest face sheet experienced more yielding, resulting in a deeper dent.

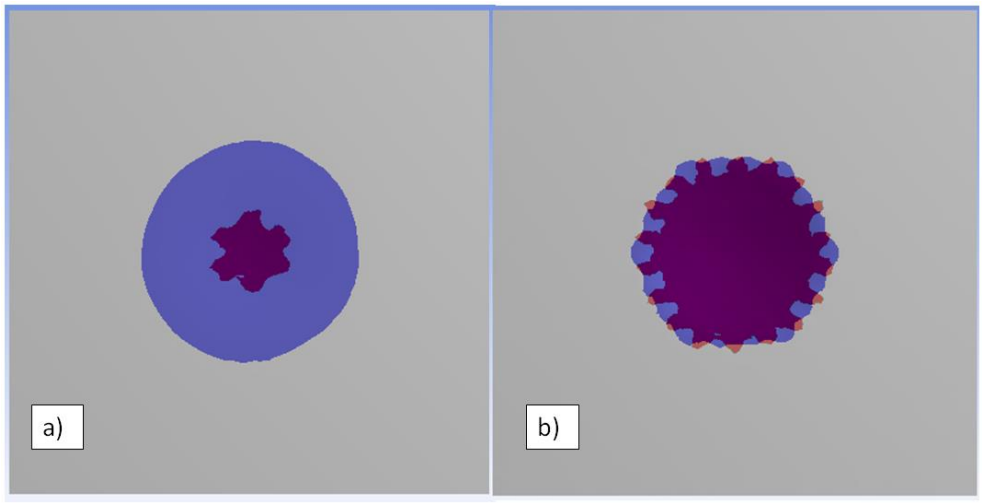

Figure 4-15: Composite image showing comparison of planar size of residual dent (in blue) and area experiencing yielding (in red) in top face sheet for impacts on sandwich panels with face sheets: a) 1.22 mm and b) 0.102 mm thick

The percentage of kinetic energy absorbed by the sandwich panel during the impact decreased linearly from 89 to 75% as the face sheet thickness was increased from 0.102 mm to 1.22 mm as seen in Figure 4-16. This shows that thicker face sheets absorb more elastic strain energy before yielding than thinner face sheets, resulting in more of the impact energy being released back to the impactor. Recall the work of Wowk & Marsden [39], who showed that a thicker face sheet resulted in a larger percentage of elastic dent spring back. As well, the thicker face sheet requires more energy to cause an equivalent amount of plastic strain, thus a thicker face sheet will be expected to see less permanent deformation and therefore a shallower dent.

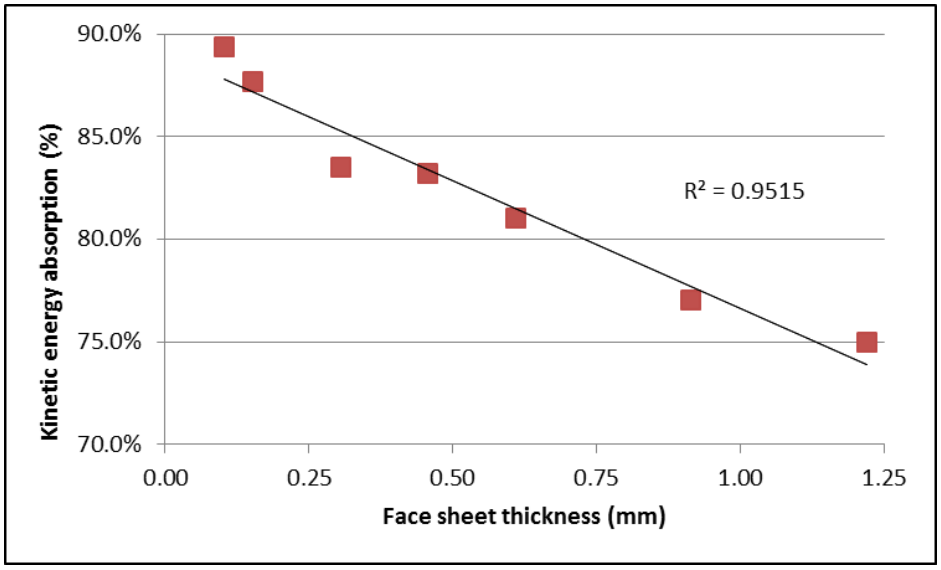

Figure 4-16: Percentage of kinetic energy absorbed during impact, as function of face sheet thickness

4.2.6. Core Density Variation

The size of the honeycomb core cells and the thickness of the cell walls were varied for this series of simulations to produce a range of core densities between 16 and 130 kg/m^3, as presented in Table 4-2. These values were selected in order to represent a wide range of readily available commercial honeycomb core configurations.

Table 4-2: Cell size, wall thickness and resultant core densities used in the core density study

Cell size, measured between parallel walls (mm, inches in brackets)	Cell wall thickness (mm, inches in brackets)	Honeycomb Core Density (kg/m^3) [3]
3.2 (1/8″)	0.051 (0.002″)	130
3.2 (1/8″)	0.025 (0.001″)	72
3.2 (1/8″)	0.018 (0.0007″)	50
4.8 (3/16″)	0.051 (0.002″)	91
4.8 (3/16″)	0.025 (0.001″)	50
4.8 (3/16″)	0.018 (0.0007″)	32
6.4 (1/4″)	0.051 (0.002″)	69
6.4 (1/4″)	0.025 (0.001″)	37
6.4 (1/4″)	0.018 (0.0007″)	26
9.5 (3/8″)	0.051(0.002″)	46
9.5 (3/8″)	0.025 (0.001″)	26
9.5 (3/8″)	0.018 (0.0007″)	16

Increasing the density of the honeycomb core resulted in a reduction in both the width and depth of the dent, as shown in Figure 4-17 and Figure 4-18, respectively, both shown with a trendline using a power function fit. Figure 4-19 shows how the aspect ratio (width / depth) of the dent varies with regard to core density, decreasing as the core density increased, with a plateau occurring beginning at 70 kg/m^3. These trends are consistent

regardless of which parameter affecting density is varied, indicating that the changes to face sheet dent shape are purely a function of the core density and not specifically cell wall thickness or cell size.

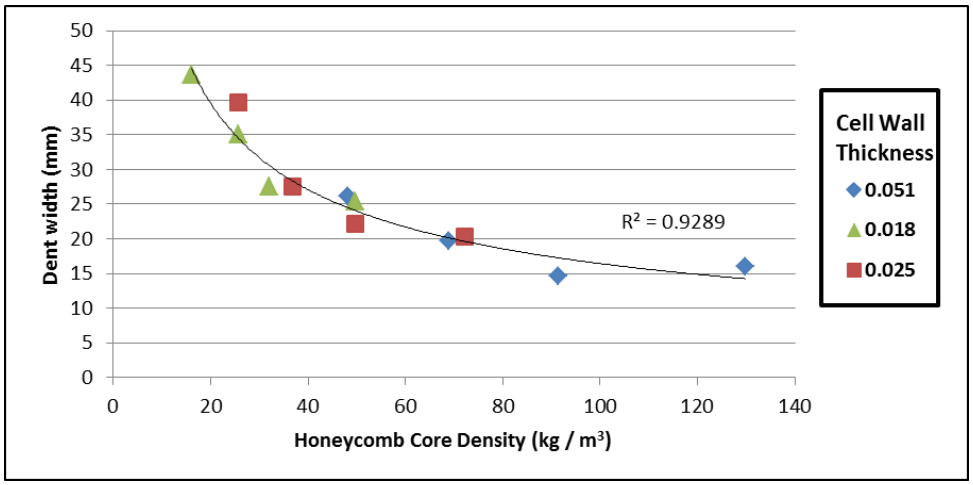

Figure 4-17: Dent width versus core density

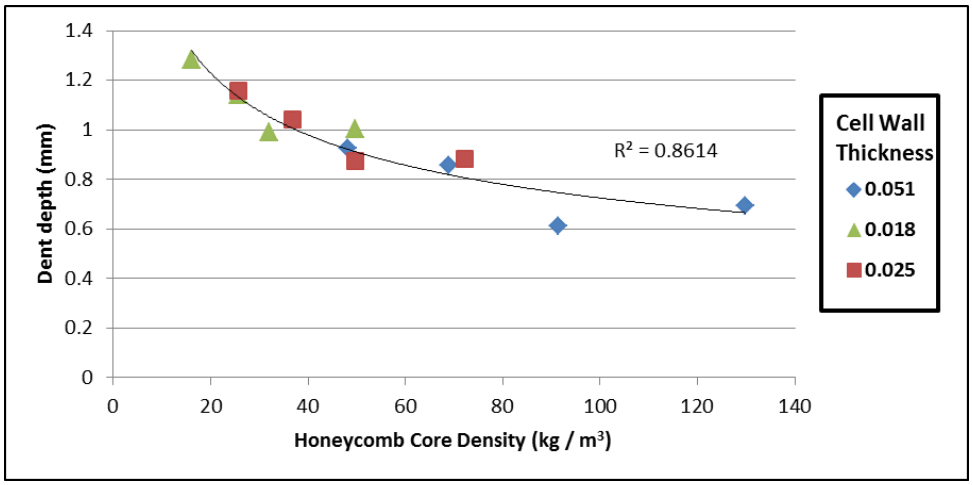

Figure 4-18: Dent depth versus core density

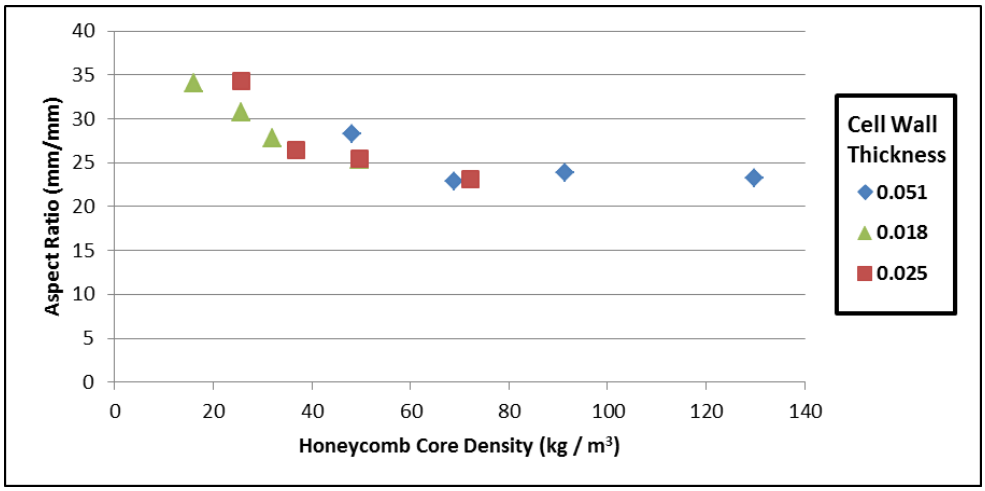

Figure 4-19: Aspect ratio variation with respect to honeycomb core density

The decrease in overall size of the dents as core density increases is a result of the increased energy absorption capacity of the denser honeycomb cores. The percentage of kinetic energy the sandwich panel absorbed during the impact increased from 70% to 90%, with increasing core density as shown in Figure 4-20. The denser cores absorbed more energy from the impact, resulting in less of the kinetic energy being retained by the impactor.

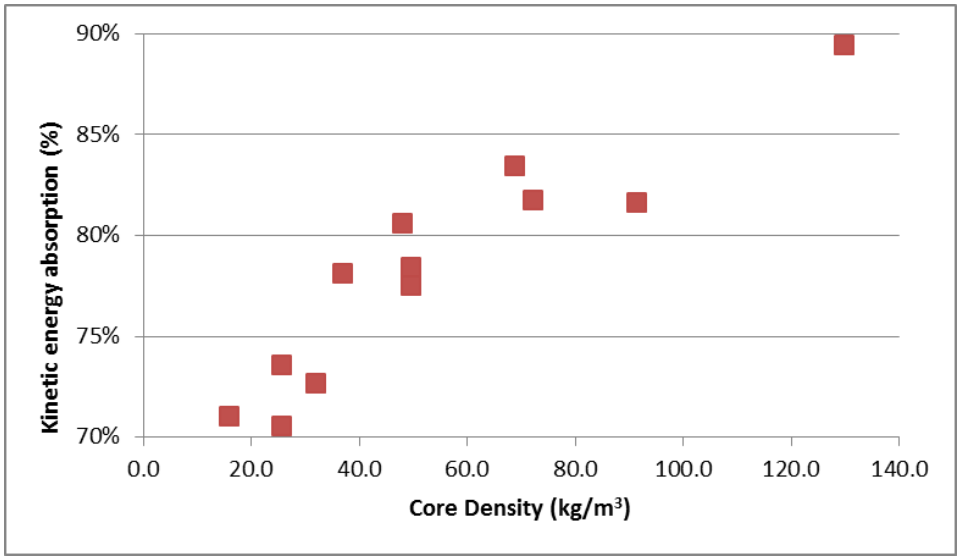

Figure 4-20: Kinetic energy absorption, as function of core density

As an impact progresses, the face sheet is deflected downwards. This results in absorbed energy being used in the permanent, plastic deformation of the core cell walls, as crushing progresses. If more energy is absorbed by the honeycomb core per unit of downward displacement of the face sheet, as is the case for a denser core, from the perspective of the impactor, this increased energy absorption results in a higher normal force resisting the impact. It slows down the impactor faster, resulting in a shorter contact time and a smaller maximum displacement. Between the least dense core and the densest core, the time of impact (the time interval over which the impactor had downward velocity) varied between 2 ms and 0.9 ms and the maximum displacement dropped from 2.37 mm to 1.04 mm. The smaller residual dent is a direct result of the reduced maximum displacement of the impactor, caused by the higher effective stiffness of the sandwich panel.

4.2.7. Surface Damage Summary

Variations in kinetic energy, core density and impactor stiffness all resulted in positive correlations between dent depth and dent width. Increases in kinetic energy and impactor stiffness resulted in larger dent depth and width and decreases in core density resulted in larger dent depth and

width. Changes to the impactor radius resulted in a negative correlation between dent depth and width, with a smaller impactor resulting in deeper and less wide dents. Varying the face sheet thickness resulted in a linear trend in the aspect ratio of width and thickness, with the ratio of width to depth increasing as the face sheet became thicker. Overall, the largest amount of surface damage was observed in the high kinetic energy simulations. Figure 4-21 shows a graph of the dent depth versus dent width for those studies mentioned.

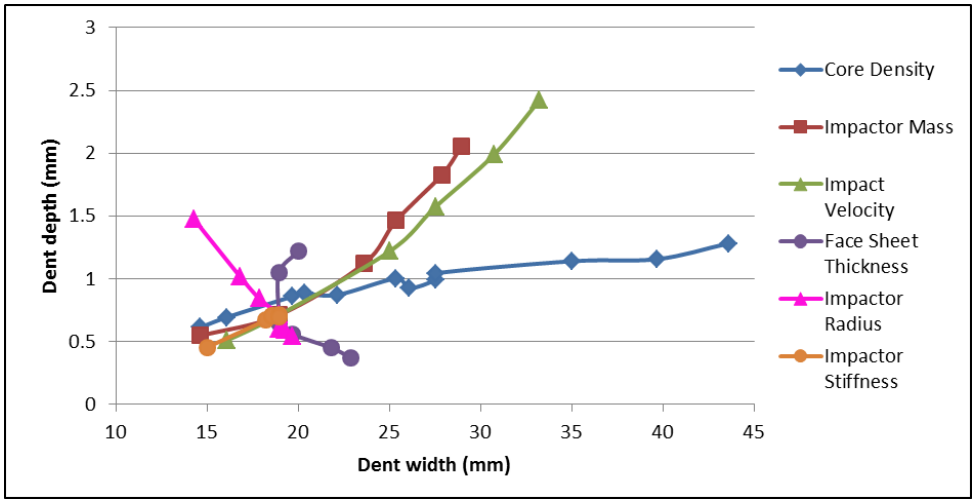

Figure 4-21: Dent depth versus dent width relationships for various simulation series

The relationship between the dent depth and the dent width presented in Figure 4-21 is not consistent between the different impact and panel parameters. This study saw dents with aspect ratios (width / depth) between 10:1 and 62:1 and it is feasible that ratios beyond that range could result using different combinations of parameters. It is not possible to determine the parameters of the impact event (impactor velocity, mass, radius or stiffness) based solely on the residual dent. In general, we can say that for a given sandwich panel, the sharper dents are likely to have been caused by a smaller object and the wider dents are likely to have been caused by either a heavier object, or a faster moving impact.

4.3. Damage to the Honeycomb Core

Damage to the honeycomb core occurred as crumpling and plastic strain in the cell walls, induced by the downward deflection of the face sheet during the impact event. This section will examine the relationship between the size of the damage created in the honeycomb core and the damage to the face sheet, as well as a specific examination of the variation of the size of the damage region when the honeycomb core density properties were varied.

4.3.1. Correlation of Width of Dent and Width of Core Damage Area

Across all simulations conducted, there was a linear relationship between the width of the residual dent in the skin and the width of the damage to the core as seen in Figure 4-22. The slope of the linear relationship is 1.05, whereas a slope of 1 indicates that the width of the core and surface damage are identical. The difference in the slopes can be attributed to rounding up the damage width measurement to the next largest cell wall, in instances where yielding only extended part of the way across a cell, as outlined in Section 3.8. The gray lines on Figure 22 indicate limits that are 3.2 mm (one cell width, for the baseline model) higher and lower than a 1:1 ratio. This indicates that the cell walls in the core experience yielding only when the face sheet above them is deformed. Therefore, the damage in the honeycomb core does not extend further than the planar area of the dent. A representative cross sectional view of the damage region is illustrated in Figure 4-23.

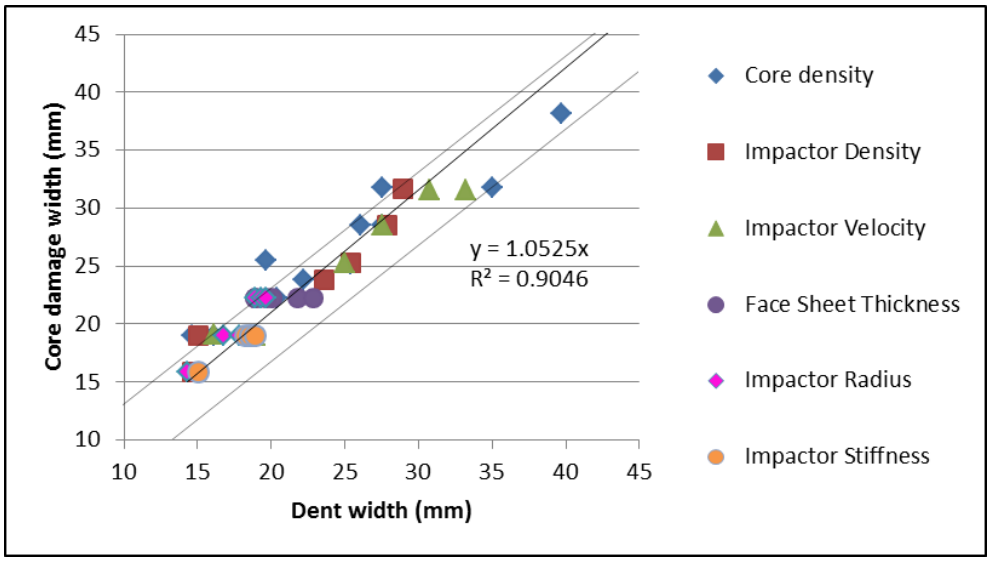

Figure 4-22: Core damage width versus dent width, for all studies. The black line is the best fit slope of 1.05, while the grey lines indicate a limit at a slope of 1, with a y intercept 3.2 mm (one cell width) above and below the x axis

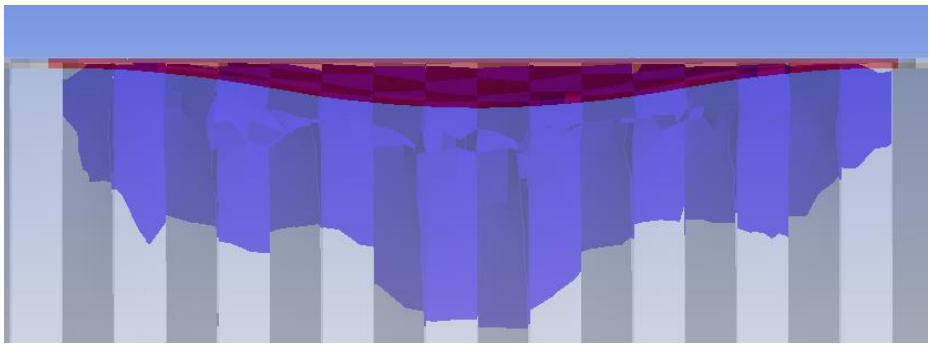

Figure 4-23: Composite image showing representative post-impact damage state, with blue indicating sections of the honeycomb core which has yielded and red indicating sections of the face sheet with a downward deflection greater than 0.01 mm

4.3.2. Depth of Core Damage

4.3.2.1. Overall Depth of Core Damage (All Current Simulations)

For all simulations completed using the baseline core density, the damage to the honeycomb core stayed within a relatively narrow band, between 5.1 to 7.0 mm, with a mean of 6.0 mm for the average depth measurement, as shown by Figure 4-24. This indicates that for a given core, as the size of planar damage area spreads, the depth of damage to the core remains constant. Thus, combined with the fact outlined in Section 4.3.1 that the width of the damage to the core matches the width of the dents, the volume of the honeycomb core damaged is solely a function of the surface area of the dent.

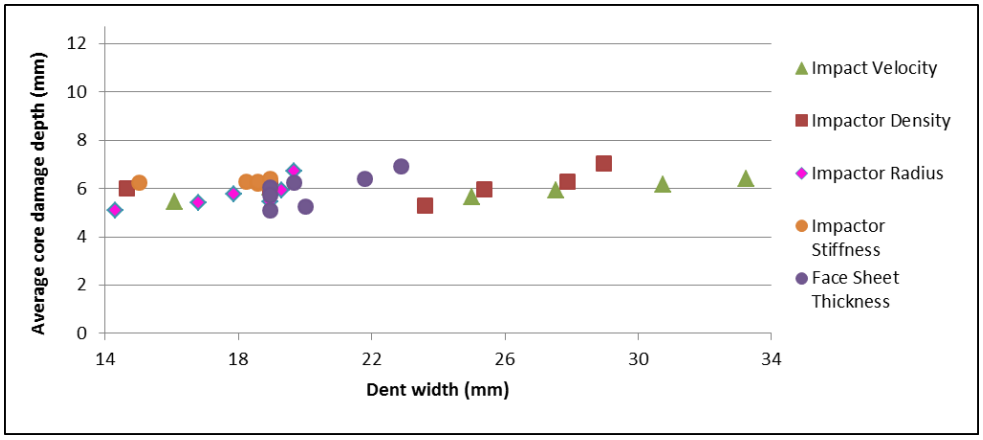

Figure 4-24: Average core damage depth versus dent width, for various studies excluding core density study

Comparing the depth of the core damage versus the depth of the dent likewise shows that the depth of the damage to the core was not influenced by the depth of the dent, as shown by Figure 4-25. Four of the simulations from the kinetic energy study did encounter a lobing phenomenon which slightly increased the average damage depth measurement. This phenomenon was an artifact of the coupon size and boundary conditions imposed and will be discussed in further detail in Section 5.2.2. These simulations have been circled in red on Figure 4-25.

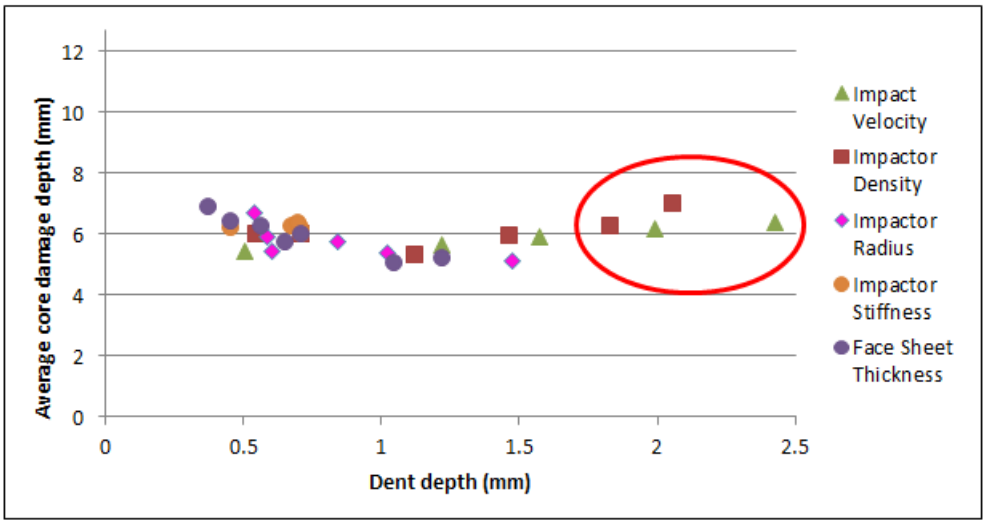

Figure 4-25: Average core damage depth versus dent depth, showing constant damage depth for all simulations using the baseline core

4.3.2.2. Core Damage Depth Variation with Core Density

When the density of the core increased, the depth of the core damage decreased as shown in Figures 4-26 and 4-27. These two figures show the same set of results, but Figure 4-26 is grouped according to different cell wall thicknesses whereas Figure 4-27 shows different cell sizes.

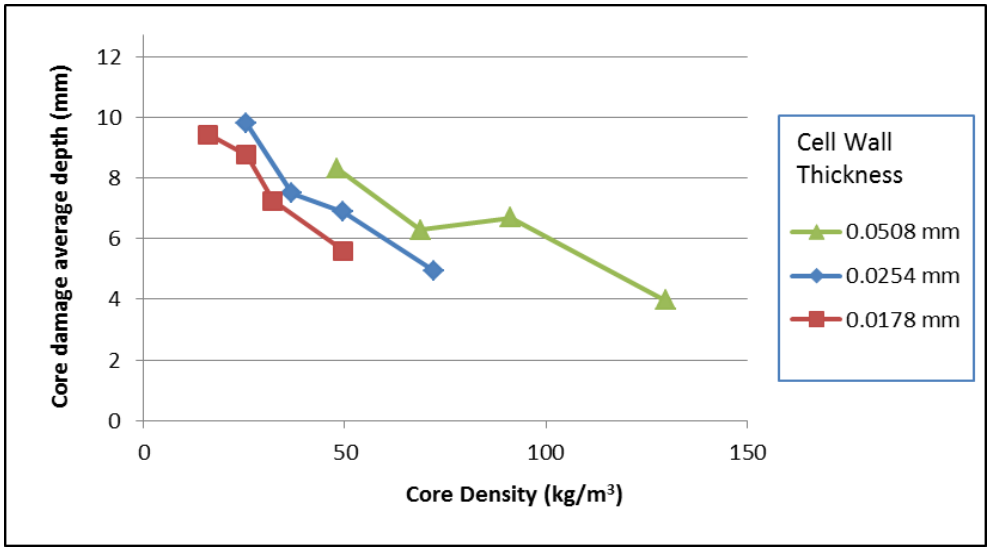

Figure 4-26: Average depth of core damage versus core density, grouped according to cell wall thickness

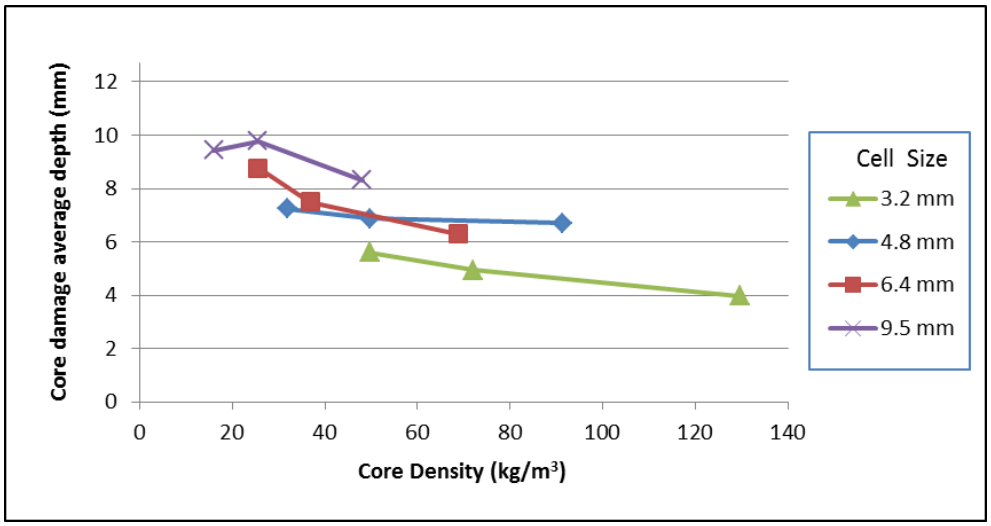

Figure 4-27: Average depth of core damage versus core density, grouped according to cell size

Changes to the cell size have a larger effect upon the depth of damage in the core. Keeping the cell wall thickness constant and reducing the cell size resulted in a decrease in core damage depth of between 40 to 52% for the

three different cell wall thicknesses examined. Conversely, keeping the cell size constant and varying the wall thickness resulted in drops between 7 and 28%. The ratio of maximum to minimum cell size is 3:1 and the ratio of maximum to minimum cell wall thickness is 2.85:1. The core damage depth decreases with increasing core density because of the effects of the increased core stiffness on the damage progression in the cell walls. Cells that are larger or have smaller wall thicknesses are more flexible and experience more displacement before crumpling occurs, therefore the depth to which the cell wall buckling occurs will be larger. The mechanism via which this occurs will be discussed further in Section 5.1.

Overall, the largest volume of damaged core will come about as a result of a less dense, less stiff core, as this will result in both a deeper core damage region and a wider planar damage area. An aircraft designer wishing to minimize damage caused by an impact may wish to select a denser core as a result, keeping in mind of course the trade-offs of increased weight and cost. Aircraft maintenance personnel who discover a dent and wish to determine the extent of damage to the honeycomb core will not need to know exactly what hit the aircraft, or how fast the impact was. The planar area of the core damage will match the planar area of the dent itself and the depth of the core damage will driven by the core density, which is known.

4.4. Panel Thickness Variation

The thickness of the panel was reduced from the baseline of 12.7 mm, to 8.89, 5.08 and 2.54 mm by decreasing the thickness of the honeycomb core. Impactor velocities were also varied between 1.5 and 4.0 m/s, in 0.5 m/s increments, while all other parameters remained unchanged from the baseline model.

It was found that the thickness of the panel had no significant effect on the damage to the panel, except when the panel became so thin that the damage to the core reached the bottom face sheet. Figure 4-28 presents the effect of core thickness on the dent depth, for all impact velocities studied. In all cases, the 2.54 mm thick panels resulted in the deepest dent. Figure 4-29 provides the resultant dent profiles for the 2.0 m/s impacts, for varying

panel thicknesses. The other velocities showed the same characteristics as in Figure 4-29.

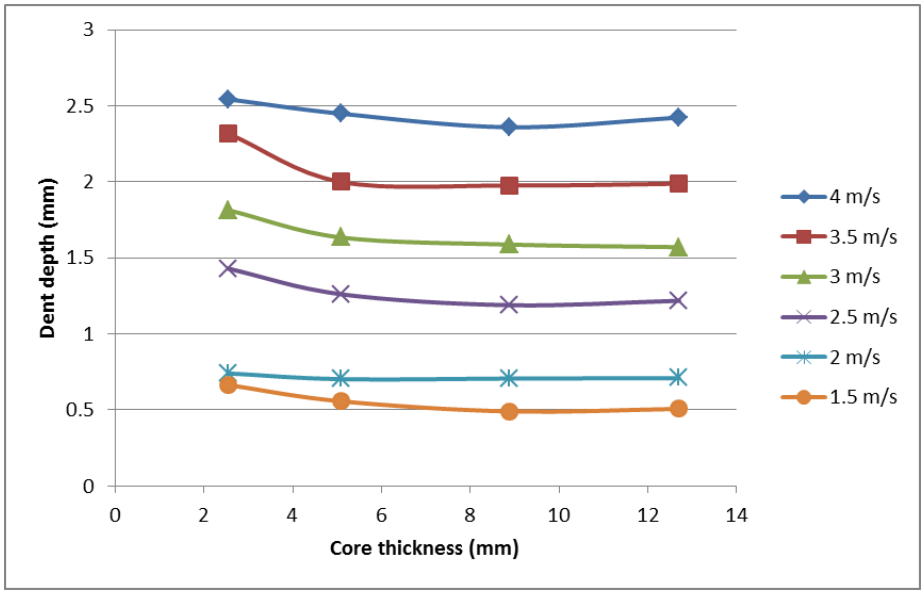

Figure 4-28: Dent depth versus core thickness, for various impact velocities

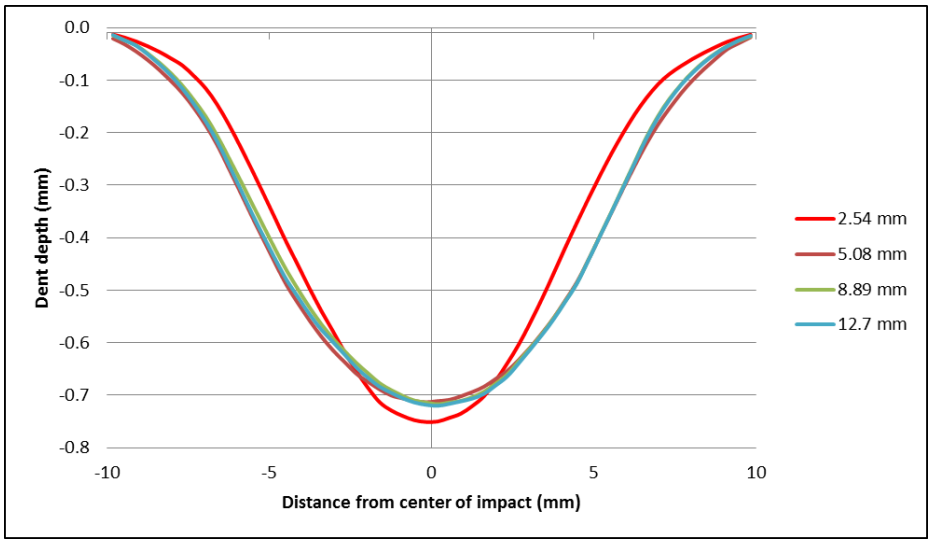

Figure 4-29: Resultant dent profile for various core thicknesses, for 2.0 m/s impact

Decreasing the panel thickness from 12.7 mm to 5.08 mm resulted in the change of the depth of the surface dent varying within a range of -1% to 9%, with an average increase of 3% for all impact velocities considered. Decreasing the panel thickness further from 5.08 mm to 2.54 mm resulted in the dent depth increases between 4 and 19%, with an average of a further 11% increase for all impact velocities considered. Changes to the size and shape of the core damage region occurred at panels thicknesses of 5.08 and 2.54 mm due to the proximity of the damage region to the bottom face sheet. Figure 4-30 shows a comparison of the damage to the honeycomb core for the various thicknesses, for the 2.0 m/s series of simulations. Similar behaviour to that in Figure 4-30 was observed for the other velocities.

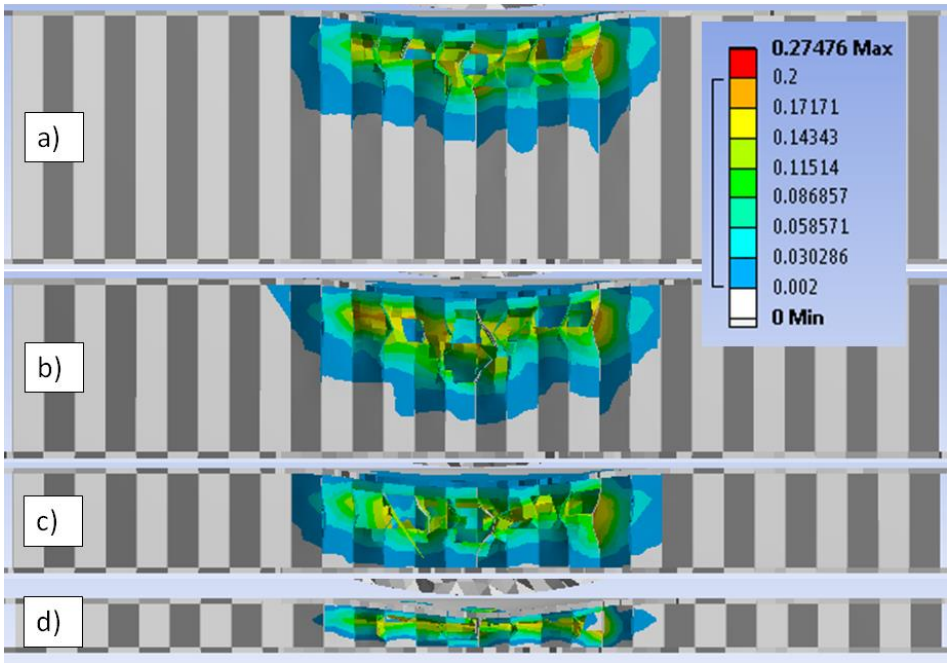

Figure 4-30: Core damage, with plastic strain indicated using scale at top right, for varying thickness, at 2 m/s impact velocity: a) 12.7mm, b) 8.89 mm, c) 5.08 mm, d) 2.54mm

5. Discussion

5.1. Core Damage Development

The average depth to which damage extends within the honeycomb core was consistently between 5.1 and 7.0 mm for all simulations involving the baseline core density. Changes in the impact velocity, impactor mass, impactor radius, impactor stiffness and face sheet thickness did not affect the depth of the core crush for a specific core density. However, when the core density was increased, the depth of the damage in the core decreased.

The explanation for the constant core damage depth for a given core density has to do with the mechanism in which a honeycomb core deforms due to an impact event. Figure 5-1 outlines the general load versus displacement behaviour of a typical honeycomb core loaded uniformly across its face by a plate, adapted from a graph provided by Hexcel, a widely used manufacturer of honeycomb products [3]. The same pattern is expected to occur locally for an impact event as well.

Initially, the honeycomb core compresses elastically with the largest stiffness that it will exhibit throughout the impact as indicated by Region 1 in Figure 5-1. Compression continues with plastic deformation and the cell walls exhibiting a wavelike pattern of displacement in the lateral directions. These lateral deflections increase and eventually buckling occurs, causing lobes (folds) to appear which coincides with the peak force that the core can resist. After buckling occurs, the load carrying capacity of the honeycomb structure drops dramatically as shown by Region 2 in Figure 5-1.

Once this drop in load occurs, one could view the honeycomb core as being composed of two separate sections; a region directly underneath the top face sheet where the cells walls have buckled and an undamaged region that still retains its rigidity below the buckled region. In the buckled region of the core, the effective stiffness has dropped to near zero as any additional displacement does not require any additional load. This is shown by the horizontal force-displacement relationship labelled as Region

3 in Figure 5-1. Any further deformation will consist of the buckled cell walls folding further until densification has occurred, where all the lobes are compacted to the point they are touching one another. During this phase, all the deformation is confined to this buckled region. Following densification of this initially damaged region of the core, the load increases again because the impact force is transmitted through the crushed honeycomb core into the undamaged core also represented in Region 3.

As new folds are formed and compacted in the section directly below the initially crushed region, a pattern of minor peaks and drops in crushing load is seen in Region 3. This progressive crushing pattern continues until the entire width of the honeycomb core has been flattened and the load increases again as shown by Region 4 in Figure 5-1. For the low velocity simulations considered in this study, only Regions 1, 2 and the first peak of Region 3 occurred.

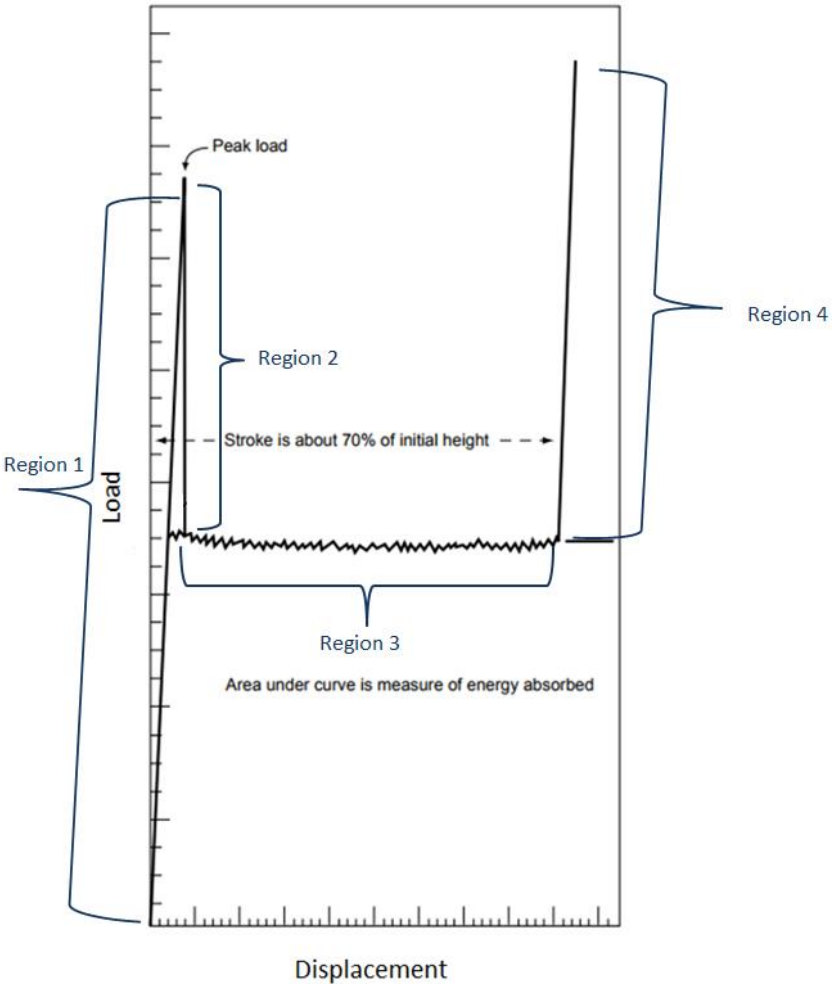

Figure 5-1: Generic aluminum honeycomb crush curve [Adapted from Reference 3]

An additional simulation was conducted in order to illustrate this progression for an impact event. A single cell of a honeycomb core, as well as half sections of the adjacent cell walls was modelled, along with the face sheets and a spherical impactor. The edges of the half-sections of the adjacent cell walls were constrained from displacing laterally away from the centre of the cell, using a cylindrical coordinate system. This simulated the stabilization that the cell walls would have from the remainder of the

honeycomb structure. Figure 5-2 shows the progression of the cell wall deformation, with the coloured regions representing plastic deformation. The amount of downward displacement of the top face sheet is indicated in each figure. Figure 5-2 a) shows the initial formation of the plastic region, followed by the formation of the wave-like pattern at the point of peak load in Figure 5-2 b). Figures 5-2 c) through e) shows the further folding of the lobes as crushing progresses to the point of maximum downward deflection. Figure 5-2 f) shows the damage state after rebound of the indenter. Throughout the crushing process, the depth of the damage remains constant once buckling has initiated.

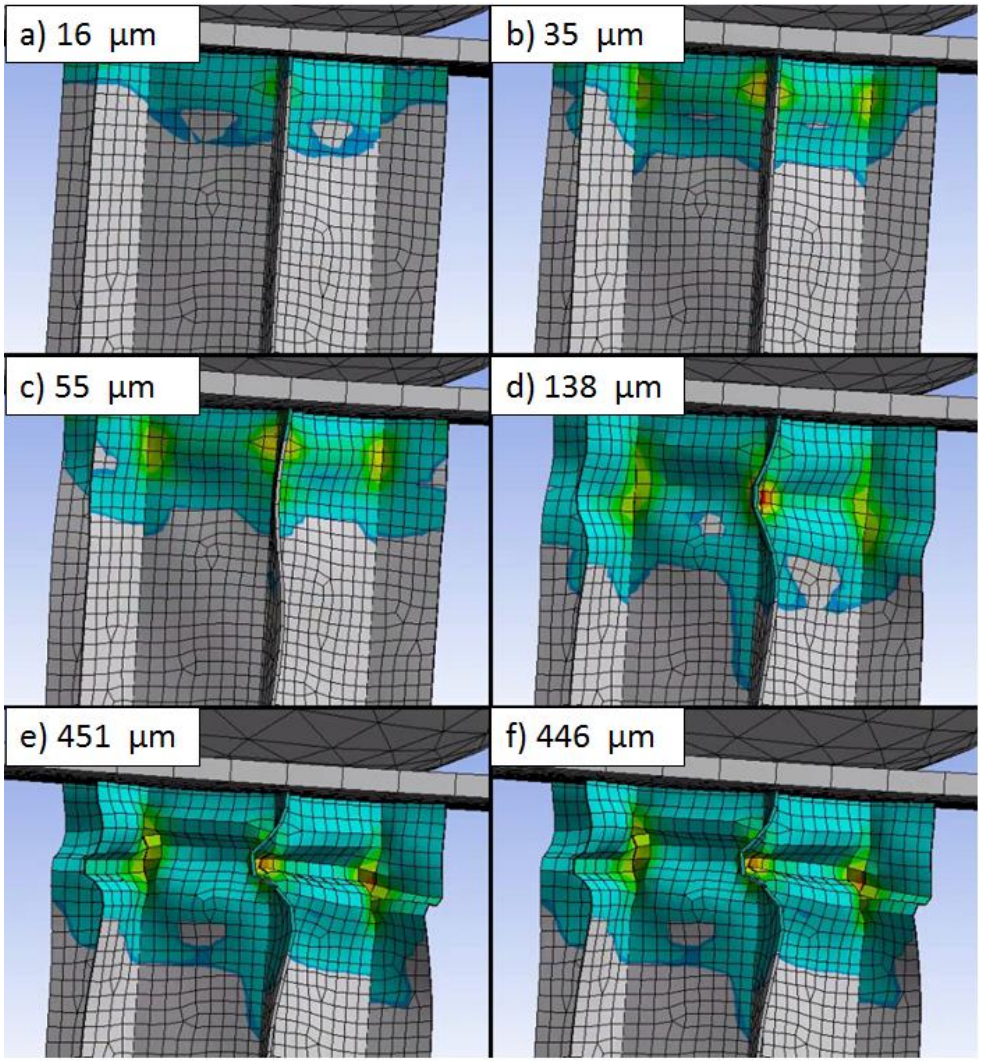

Figure 5-2: Progression of impact damage on single honeycomb cell with a 37mJ impact energy, with light blue indicating the onset of yielding and red indicating the sections of highest plastic strain

It is the initial formation and shape of the wavelike pattern which occurs after buckling has initiated in Figure 5-2 b) that determines what the depth of the core damage will be. Once buckling has started, any further downward deflection of the face sheet crushes the already damaged section causing the lobes to fold flatter. Damage is confined to this section only,

because the stiffness of the buckled region is substantially lower than the stiffness of the undamaged section.

This is supported by the work of Zhao and Gary [24] who outlined how a honeycomb core which has a pre-damaged section will not experience the high peak load that an undamaged honeycomb core will. The damaged section will be the first section to be crushed and because it has a lower resistance to deformation, it will crush at a lower load than an undamaged core.

If an impact is severe enough to cause densification of the initial crushed core region, damage will then continue progressively, with small sections of the honeycomb core buckling, folding in on itself and once again becoming stiff enough that enough force is passed through it to initiate damage in a new segment of the honeycomb core. In order to illustrate this, a simulation was conducted similar to the one outlined in Figure 5-2, except the impactor used had 4 times the mass of the initial simulation (34 g versus 8.4g). Figure 5-3 outlines the crushing progression during this more severe impact. The initial damage pattern is similar in size and shape to the damage patterns seen at similar displacement levels for the first simulation. In Figure 5-3 e), at 1.3 mm of displacement, densification of the initial damage region had occurred. The impact energy is still sufficient to continue to damage the core and in Figures 5-3 f) through g) more buckling lobes form below the densified region.

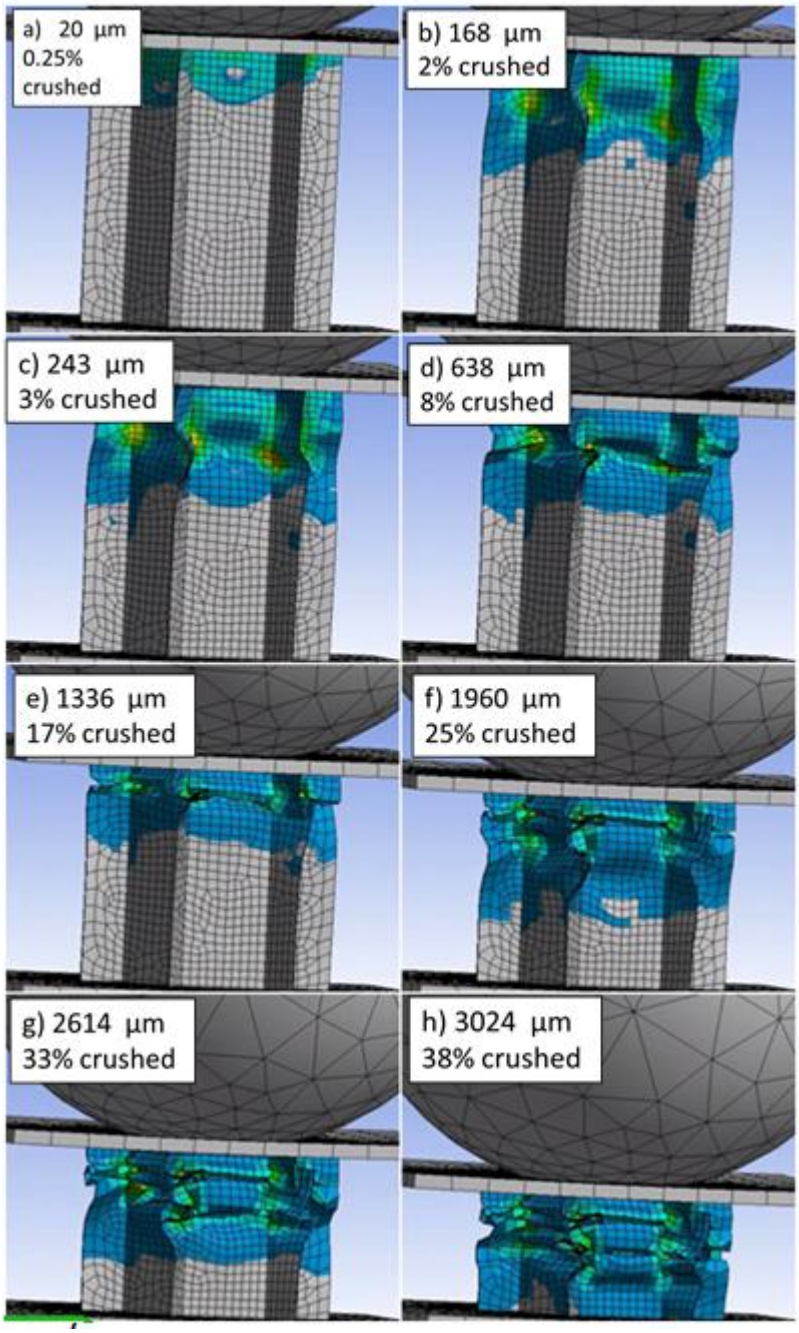

Figure 5-3: Progression of impact damage on single honeycomb cell, with a 151 mJ impact energy, with light blue indicating the onset of yielding and red indicating the sections of highest plastic strain

As the initial formation of the wavelike displacement, which eventually leads to buckling and crushing, occurs almost immediately after impact, neither the maximum dent depth nor the final residual dent depth have any influence upon the depth of this initial section of damaged core. Therefore, any variables which may have an influence upon the shape of the residual dent, such as the impact energy, the impactor size, the face sheet thickness, impactor stiffness, etc., will not have any effect upon the depth of this initial damage region. The only parameter which was shown to have an influence on this effect is the density of the honeycomb core itself.

This does not mean that the damage to the honeycomb core is always constant. The sandwich panel can experience a strong enough impact that the honeycomb core will undergo densification, resulting in the damage region being pushed deeper than the initially damaged section. Any impact producing BVID will not experience this phenomenon. For such dents, the depth to which the honeycomb core is damaged can be viewed as constant. The impacts presented in Section 4.3.2 of this thesis were not severe enough to cause densification of the initial damage region, therefore the depth of the core damage was consistent across all simulations with constant honeycomb core properties. Figure 5-4 provides some examples from the work of Reyno [32], showing cross sections of honeycomb panels with BVID. These six examples show the consistent damage depth across the width of the dent that was predicted through the finite element analyses presented in Section 4.3.2.1. These cores do not show signs of densification, lacking the distinct pattern of the cell walls folding in upon themselves.

Figure 5-4: Crumpling of honeycomb core in cross sectioned dented aluminum-aluminum honeycomb sandwich panels [Adapted from Reference 32]

It should be cautioned that these results should only be considered valid for honeycomb cores which fail via the ductile folding and crushing pattern discussed above. This will generally be limited to metallic honeycomb cores. Nomex™ honeycomb cores are quite commonly used in aerospace applications, but being a less ductile material than aluminum, Nomex honeycomb cores often fail via brittle fracture or cracking. The wavelike pattern previously discussed does not form in the honeycomb, which results in the initial damage region not being limited to the area immediately beneath the impact. Figure 5-5 shows a comparison of the damage patterns observed by Aminanda *et al.* [28] between the two materials.

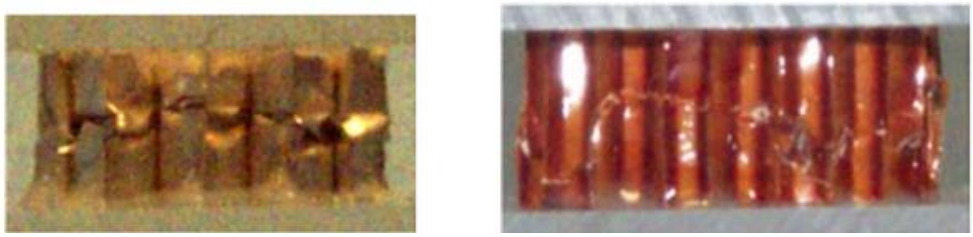

Figure 5-5: Comparison of crushing behaviour of compacted aluminum and Nomex™ honeycomb cores [Adapted from Reference 28]

5.2. Core Damage Shape

5.2.1. Overall Shape of Core Damage Region

The majority of simulations conducted showed a triangular shape to the damage pattern in the honeycomb core. The largest damage depth occurred underneath the center of the impact area and tapered off at the edge of the dent. Figure 5-6 shows an example of one such impact exhibiting this pattern.

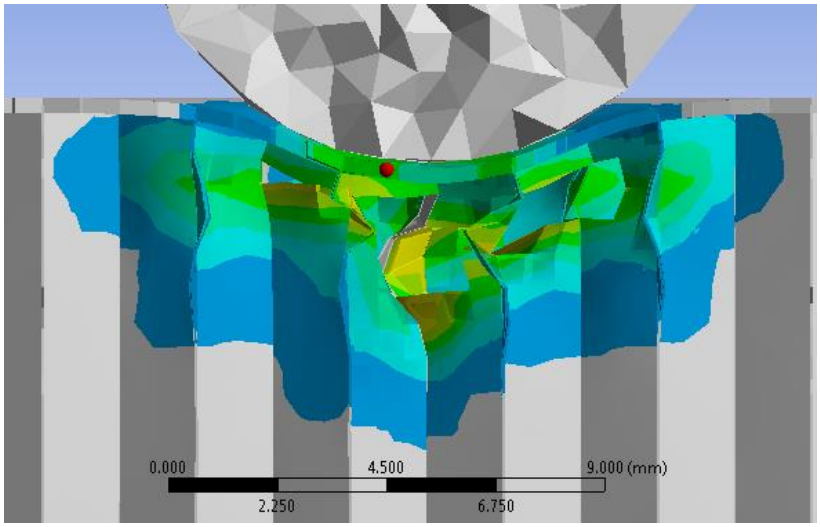

Figure 5-6: Honeycomb core damage region showing a triangular pattern from the 6.35 mm radius impactor, with light blue indicating the onset of yielding and yellow indicating the sections of highest plastic strain

The triangular shape of the damaged core is a result of the mesh sizing. Honeycomb core with a coarser mesh will effectively be stiffer than a finer mesh because it has fewer degrees of freedom. For example, a finer meshed core will be able to fold in upon itself multiple times, whereas a coarser mesh may be only able to form one fold. When a very fine mesh is used, a buckled cell wall acts more independently and has a smaller effect on the effectiveness stiffness of adjacent cell walls. The core damage region appears more rectangular in shape because buckling is only initiated by deformation of the skin rather than adjacent cells.

To demonstrate this, simulations were conducted using a finer mesh sizing of 0.3 mm instead of the 0.76 mm used for the simulations in Chapter 4. The finer mesh increased the number of elements across a cell wall from 3 to 7 and resulted in a rectangular core damage region rather than the triangular shape. Figure 5-7 illustrates a comparison of a 1.5 m/s impact using baseline parameters for both mesh sizes, shown at the same magnification.

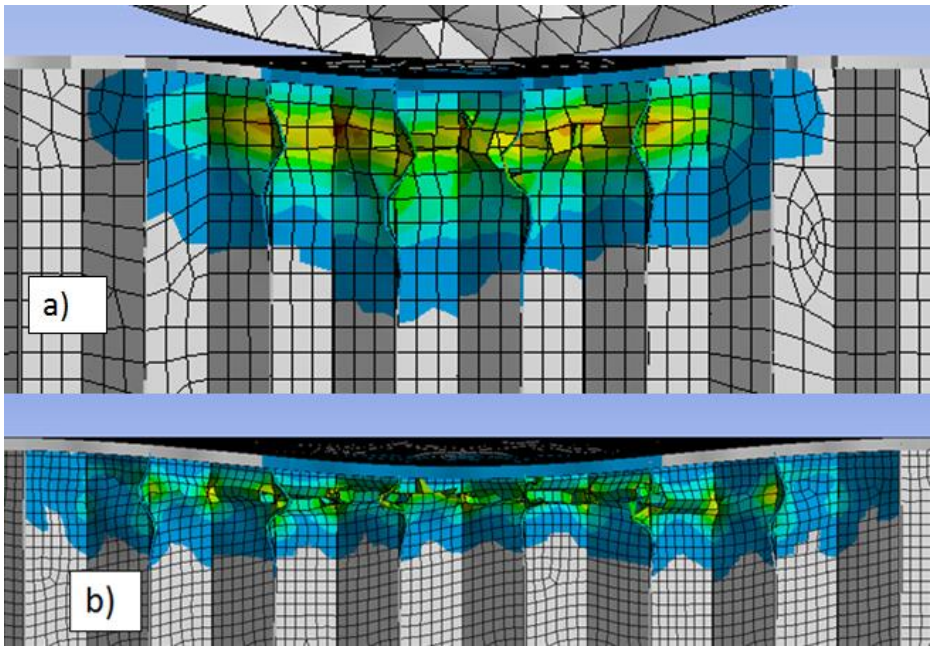

Figure 5-7: A comparison of the honeycomb core damage region, using the same scale, for a 1.5 m/s impact, between: a) a coarse meshed model and b) a fine meshed model, with light blue indicating the onset of yielding and red indicating the sections of highest plastic strain

The two primary effects of the finer mesh can be seen in Figure 5-7; the finer mesh allows for more buckling modes, which reduces the depth to which the damage extends and the reduced effective stiffness of the honeycomb core in the finer mesh also absorbs less energy during the impact, causing a larger portion of the energy of the impact being used to deform the face sheet, which results in a deeper and wider dent. In the fine-meshed simulation, the residual dent depth was 24% larger (0.723 mm versus 0.584 mm) and the residual dent width was 31% larger (22.5 mm versus 17.2 mm) than the simulation with the coarser mesh, with all other parameters being equal. For the core damage, the average depth was 45% lower (2.98 mm versus 5.44) and the width was 16% larger (22.2 mm versus 19.1 mm) in the fine meshed model. Because of this reduced stiffness, the contact time was also longer, with the maximum downward displacement occurring at 1.43 ms versus 1.08 ms in the model with the coarser mesh. The damage pattern is much more consistent, with the ratio between the maximum depth and the average depth of the damage being only 1.17, versus 1.36 for the coarser mesh. While changing the mesh size did change the measurements of the damage created, the overall observed trends in damage patterns remained the same. The pattern of damage depth being constant was the same and the trend of the aspect ratio for surface damage was not affected. Based upon the analysis presented in Section 5.1, a rectangular core damage cross section pattern is expected, rather than the triangular pattern which is an artifact of the mesh sizing.

As it is the buckling phenomenon which causes the constant depth of damage phenomenon, near the edges of the damage region where downward deflection of the face sheet is not sufficient to initiate buckling, a smaller damage depth will be expected. The threshold used throughout this study for the point at which the surface dent starts is when the downward deflection exceeds 0.01 mm, or 10 μm. As seen in Figures 5-2 and 5-3, this amount of deflection would be enough to start the onset of plastic deformation in the honeycomb core, but would not be enough to initiate crumpling or to cause the plastic deformation to reach the full depth to which it will end up extending. Therefore, some tapering of the depth of the honeycomb core damage region can be expected near the edges of a dent. This can be seen in Figure 5-7, where the damage region within the two outermost cells does not extend as deep on the outer sides

of the cell walls as it does on the inner sides of the cell walls. Buckling is occurring along the edge where those cell walls meet the adjacent inner cell walls, but the damage region on the outer edge of the two cell walls is caused by downward deflection below the threshold required to initiate crumpling. Thus the damage does not extend as deep as it would have had buckling occurred along the outmost edges.

5.2.2. Side Lobes in Core Damage Region

Some of the higher energy impacts showed a damage region with a relatively flat section of damage in the centre and lobes on the outside edges where the damage region extends deeper. An example of this is shown in Figure 5-8. This phenomenon causes the rise in the average core damage depth observed for the highest energy impacts in the Kinetic Energy Variation study, which was mentioned in in Section 4.3.2.1.

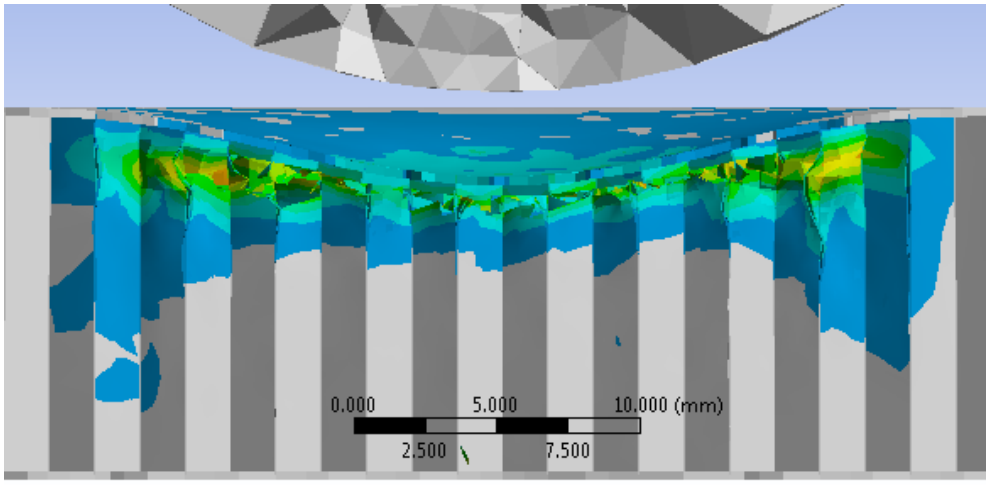

Figure 5-8: Side lobe pattern of honeycomb core damage for the 4.0 m/s impact, with light blue indicating the onset of yielding and red indicating the sections of highest plastic strain

Two factors contributed towards this phenomenon; the size distribution of the elements as well as the size of the panel. The mesh used for the baseline model, as seen in Figure 3-4, had a finer mesh in the expected damage region for improved accuracy and a coarser mesh for the remaining core in order to reduce computational run times. For the baseline model, the

damage was contained to the region with the fine mesh, for but for some high energy impacts, the damage region extended into the coarser mesh. As previously discussed in Section 5.2.1 the depth of the core damage region increases with a coarser mesh resulting in deeper core damage in the larger elements. Figure 5-9 shows an example of this effect, for the 4.0 m/s impact with baseline parameters. The influence of the different mesh regions (outlined in orange) on the damage depth are clearly visible.

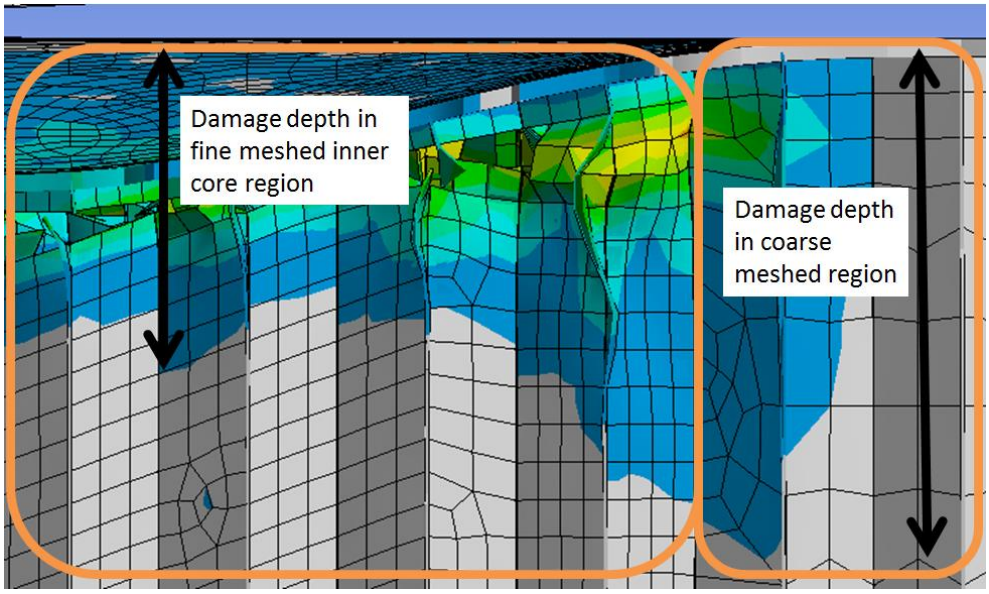

Figure 5-9: Damage extending into the coarse mesh results in deeper core damage at the outer regions of the dent, with light blue indicating the onset of yielding and yellow indicating the sections of highest plastic strain

A simulation of a 3.0m/s impact was conducted with uniform mesh sizing of 0.3 mm throughout the entire core in an attempt to eliminate the lobes at the edges of the dent. Figure 5-10 shows that the lobes were still present, indicating that this effect could not be wholly explained by the coarse mesh sizing.

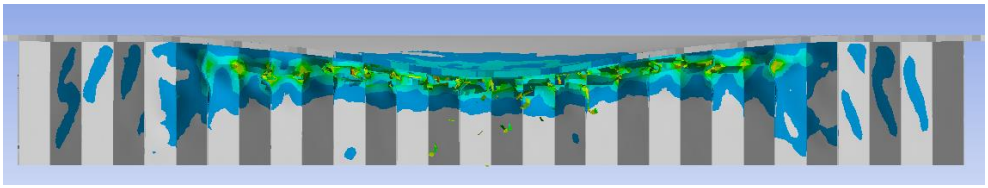

Figure 5-10: Honeycomb core damage pattern for 3.0 m/s impact, using a mesh sizing of 0.3mm, with light blue indicating the onset of yielding and yellow indicating the sections of highest plastic strain

The second factor which contributed towards this phenomenon was the edges of the panel pulling inwards towards the dent. Figure 5-11 illustrates that even with the finer mesh the in-plane displacement of the top face sheet extends all the way to the edges of the panel, even though the vertical displacement is confined to the dent region. In both instances coloured areas indicate displacement greater than 0.01 mm. This shows that the absence of constraints on the edges of the panel allows the core and the top face sheet to be drawn inwards towards the dent.

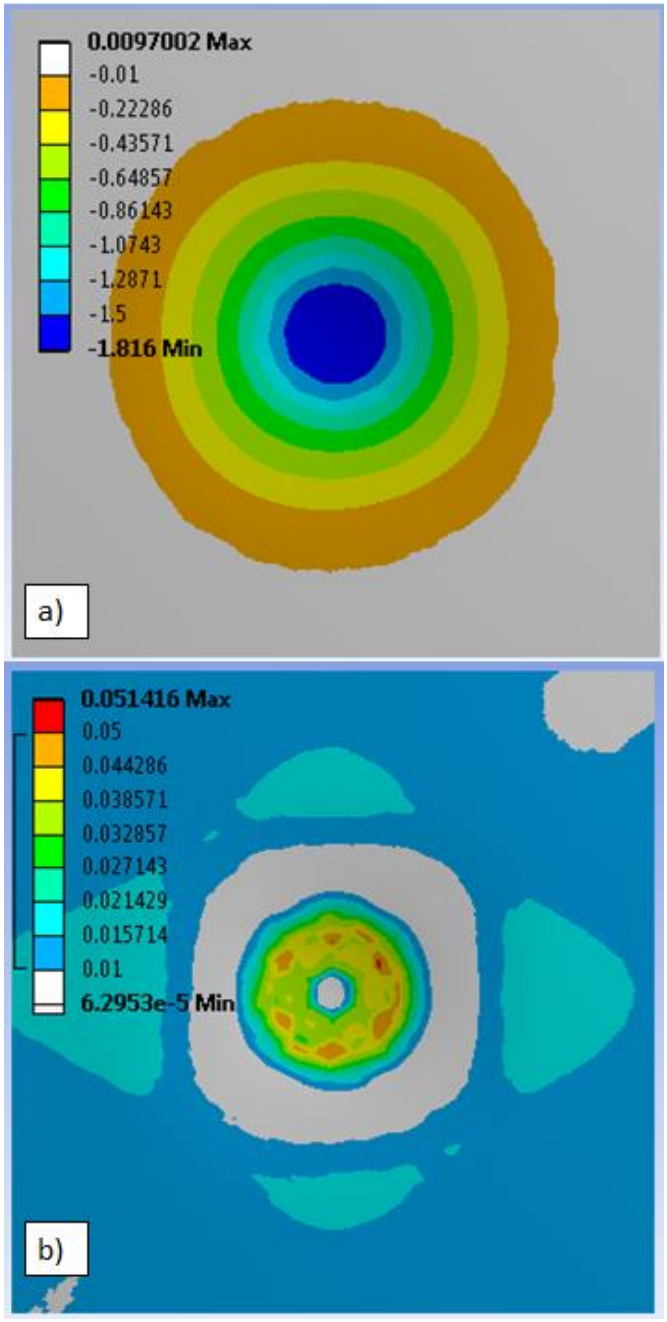

Figure 5-11: Comparison of a) vertical and b) in-plane displacement in mm of the top face sheet, for the 3.0 m/s impact with an element size of 0.3 mm.

While this may be an effect which can realistically occur during coupon-level testing, in any full sized sandwich panel the face sheet and core will be constrained by adjacent cells and will not allow for significant in-plane deflection. In order to model this, a simulation was conducted which had both a uniform mesh sizing in the core and boundary conditions applied to the outward edges of the face sheet and honeycomb core which prevented any in-plane movement. The edges to which these boundaries were applied were at least 5 cells away from the surface dent, thus this boundary condition would not prevent any crumpling of the core.

Fixing the edges of the top face sheet and the edges of the core from lateral displacement completely eliminated the in-plane movement. Figure 5-12 b) shows that the in-plane displacement was confined only to the dent itself.

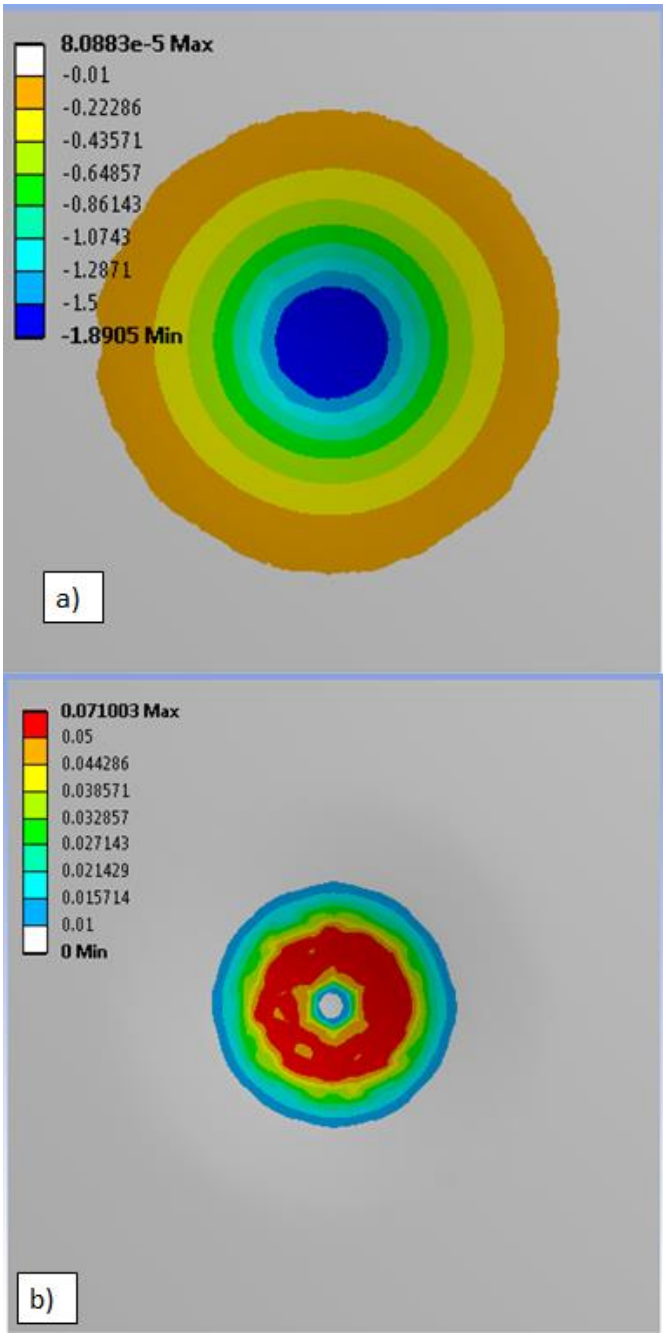

Figure 5-12: Comparison of a) vertical and b) in-plane displacement in mm of the upper face sheet, for a 3.0 m/s impact with an element size of 0.3mm and edge boundary conditions imposed

Figure 5-13 shows the progression of the damage in the honeycomb core and that by completely removing the in-place displacement of the face sheet and the core, the lobing effect was also eliminated. The core damage showed a rectangular shape which was typical of the lower energy impacts from 4.3.2. The imposition of the edge constraints had minimal effect upon the residual dent size, increasing the residual dent depth by 4% and decreasing the dent width by 3%.

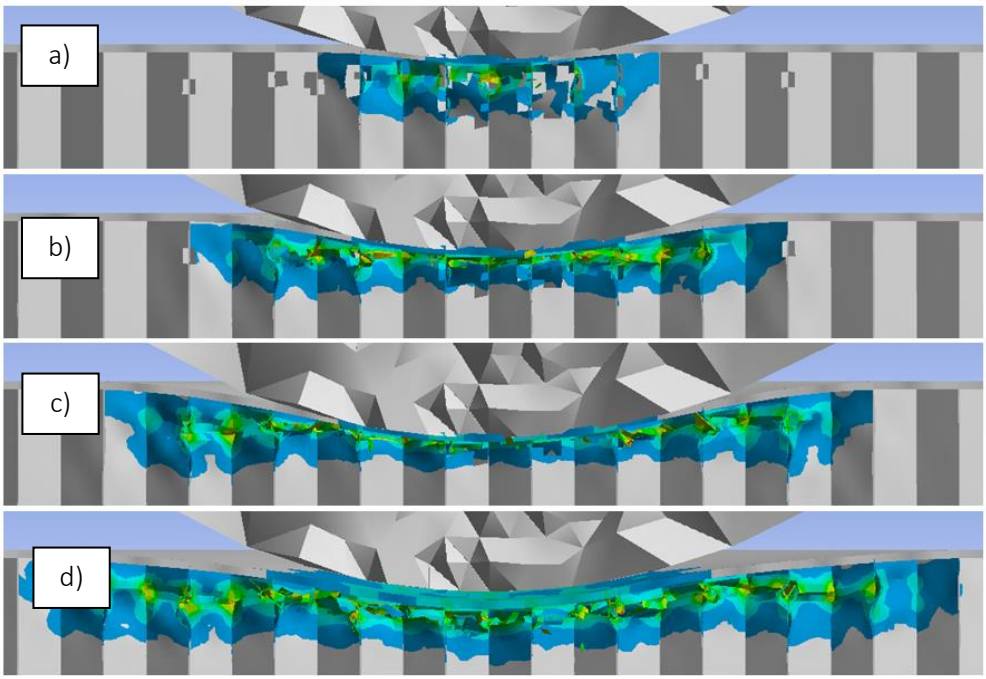

Figure 5-13: Development of honeycomb core damage pattern for 3.0 m/s impact, using a mesh sizing of 0.3mm with edge boundary conditions imposed, with light blue indicating the onset of yielding and yellow indicating the sections of highest plastic strain

With a uniform mesh sizing and the edges constrained, the core damage develops in the same manner as discussed in Section 5.1. The expected damage pattern is a rectangular region, with no lobes and a protruding section below the impact in instances where the crushing of the honeycomb core was severe enough to induce densification.

5.3. Mesh Sizing

It has been shown that the sizing of the mesh in the honeycomb core has an effect on the damage characteristics measured, with a finer mesh leading to a deeper and wider dent and a shallower and wider core damage region. A coarser mesh is less free to deform, with an effective higher local stiffness, resulting in the damage region extending deeper into the core. Consider a two dimensional bar element which rotates in order to accommodate axial displacement at its end points. A mesh of longer bars will have the lateral displacement occurring further from the loaded end than a fine mesh as illustrated in Figure 5-14. The coarse mesh will therefore result in a larger modelled damage depth, but the surface dent will be shallower and less wide due to the artificially increased stiffness.

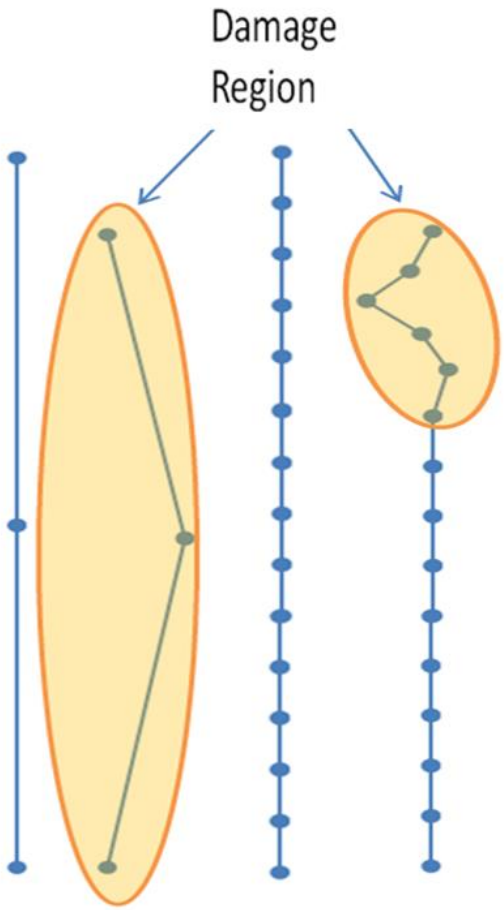

Figure 5-14: Illustration of how mesh sizing restricts available options for deformation, resulting in a larger measured damage region

5.4. Applicability to Modelling of Residual Strength

In order to accurately model the effect that impact damage has on the residual strength and stiffness of honeycomb sandwich panels with low velocity impact damage, the depth and width of the damage region must be known, as shown by Horrigan & Staal [46], who determined that the critical load causing face sheet wrinkling leading to buckling was a function of the planar size and depth of the damage region. The impact

simulations with the mesh size of (0.3 mm) took between 36 and 53 hours to run, using a computer system with a deca-core 2.30 GHz processor with 18 GB of RAM. This would have to be followed by a subsequent analysis in order to predict residual strength. However, a simulation of the impact event does not need to be conducted for every set of impact parameters because it is expected that the depth of the core damage is constant and the width of the damage is confined to the width of the dent. The size of the damage region could potentially be predicted as long as the core density is known. If the size of the damage region in the honeycomb core is known, it could be modelled as a flat puck with a known constant depth and whose width is equal to that of the residual dent. This representation, shown in Figure 5-15 could be used in a simplified model of the panel, in which the honeycomb core is replaced by a homogenous material with orthotropic stiffness equivalent to that of the undamaged core. The puck representing the damaged core could be defined as having a decreased stiffness compared to the undamaged core, similar to the approach outlined by James, Watson and Cunningham [50]. The after-impact residual strength and stiffness of the honeycomb panel could then be modelled.

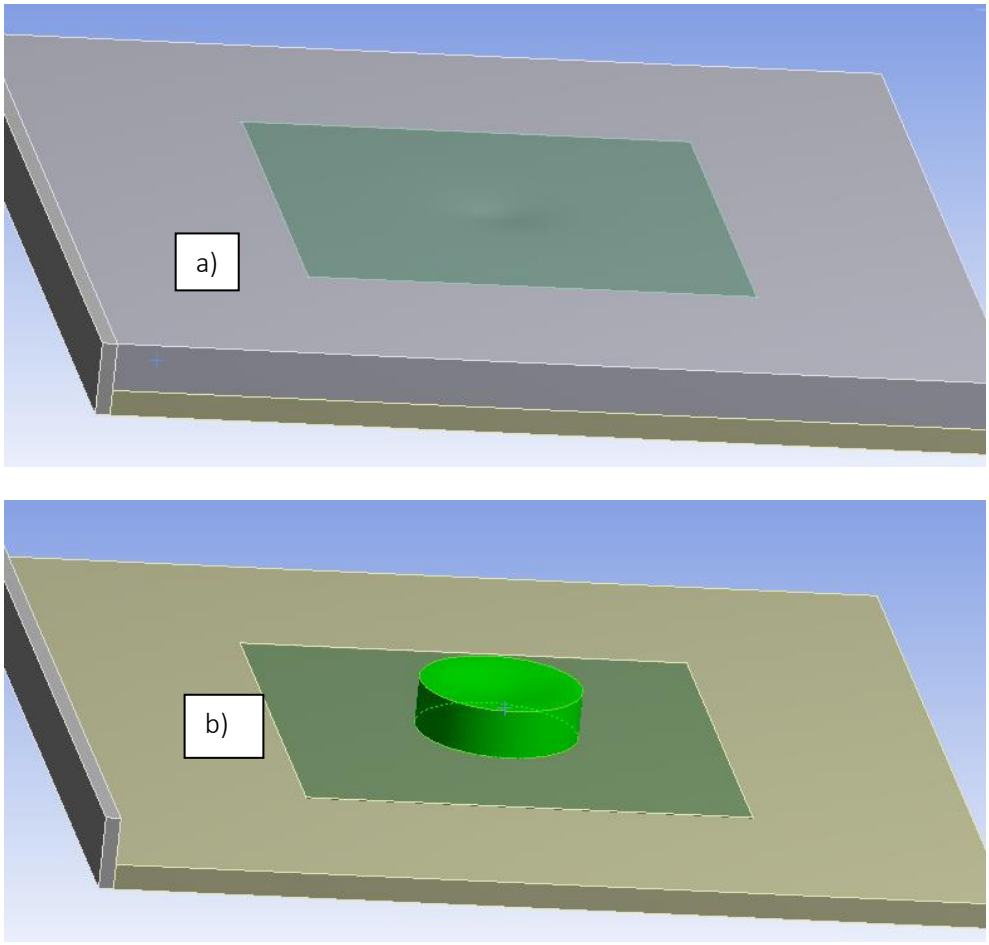

Figure 5-15: Simplified model of honeycomb sandwich panel, showing a) the dent following an impact analysis and b) a representation of the damaged core by a puck with adjusted material properties, with the top face sheet and remainder the honeycomb core around the damage section hidden in order to highlight the damaged section

6. Conclusions

A systematic approach was taken to investigate the correlations that exist between a residual surface dent and underlying damage during a low-velocity impact event on an aluminum-aluminum honeycomb sandwich panel. Finite element analysis was conducted in order to allow for simulations of impact tests covering a wide range of different types of panels and impacts with different parameters. Damage was quantified on the basis of the size and shape of the resultant dent and of the region of the honeycomb core damaged during the impact event. Impacts examined resulted in BVID and VID as well as some damage above the allowable limits for panels used in the RCAF's Griffon helicopters. Key conclusions were:

a) The width of the core damage did not extend significantly beyond the residual dent in the face sheet. The overall relationship between dent width and core damage width was linear.

b) The residual dent aspect ratio is not constant across each study, which means that the impact parameters couldn't be deduced based solely upon the width and depth of the dent.

c) The average depths of the core damage were relatively constant for all studies using the baseline core density, when the velocity, impactor mass, impactor radius, impactor stiffness and face sheet thickness were varied. However, the depth of the core damage was dependent on the density of the honeycomb core and when the core density was decreased the core damage depth increased.

d) Varying the panel thickness had negligible effects upon the residual dent in the face sheet for all but the set of simulations on extremely thin panels, which resulted in a deeper dent profile and thorough crushing (densification) of the honeycomb core underneath the impact area.

e) Mesh sizing has a strong influence upon the depth to which core damage will occur in a simulation. Using a coarser mesh will overestimate the depth to which core damage reaches, but will underestimate the depth and

width of the surface dent. A fine mesh should be used when determining the depth to which damage propagates, which can in turn be used to predict the damage underneath a dent of known size and shape.

f) When conducting or simulating impact testing, either the edges of the panel should be constrained, or the panel should be large enough to restrain overall inward displacement of the face sheet being impacted, in order to avoid damage to the honeycomb core by lateral displacement that would not otherwise occur in a full size panel, attached to the remaining structure of an aircraft.

6.1. Future Work

Based upon the research presented in this study, recommended topics for future research are as follows:

This research did not cover the effect of low-velocity impacts on curved honeycomb sandwich panels, sandwich panels with non-zero wall partition angles, impacts at an angle and events involving non-spherical impactors. Research should be conducted to determine what effect, if any, these variables may have upon the validity of the conclusions drawn in this study.

Experimental validation of these results should be conducted, in order to meet airworthiness certification requirements when using the conclusions drawn.

Nomex™ is increasingly widely used in lieu of aluminum for the construction of honeycomb cores. As it has more of a tendency to fail via fracture, rather than the folding and crumpling behaviour seen in aluminum honeycombs, the results of this research cannot be assumed to be directly applicable to Nomex™ cores. There remains a relative lack of research into the depth to which damage tends to propagate in Nomex™ cores during low-velocity impacts and further study is warranted.

Finally, investigation into aluminum honeycomb sandwich panels with non-aluminum face sheets (especially the types of carbon fibre reinforced polymer or other composite material face sheets being increasingly used in aircraft design and manufacture) should be conducted, to determine to what degree the results of this study are valid for face sheets with different impact response characteristics.

7. Bibliography

[1] Aktay, L., Johnson, A, & Kröplin, B. (2008). Numerical modelling of honeycomb core crush behaviour. *Engineering Fracture Mechanics*, *75 (9), pp.* 2616-2630.

[2] The Fibre Reinforced Plastic & Composite Technology Resource Centre (2010, December 12). *Sandwich Composite and Core Material*. [Web log post] Retrieved from fibre-reinforced-plastic.com/2010/12/sandwich-composite-and-core-material.html, accessed 19 Oct 2017.

[3] Hexcel Corporation (2016). *HexWeb® Honeycomb Attributes and Properties.* Retrieved from the Hexcel website hexcel.com/Products/Honeycomb/, accessed 17 Oct 2017.

[4] Feraboli, P. (2006). Some recommendations for characterization of composite panels by means of drop tower impact testing. *Journal of Aircraft*, *43 (6),* pp. 1710-1718.

[5] Prior, S. (2016) *Characterization of Sandwich Panels Subject to Low-Velocity Impact*. Thesis, Royal Military College of Canada.

[6] United States Federal Aviation Administration. (2009, September 08). Advisory Circular 20-107B - Composite Aircraft Structure.

[7] Fawcett, A., & Oakes, G. Boeing Composite Airframe Damage Tolerance and Service Experience. [Powerpoint Presentation] Retrieved from servidor-da.aero.upm.es/wip/apuntes/quinto/materiales-compuestos/tolerancia%20al%20dano.pdf.pdf, accessed 19 Oct, 2017.

[8] Reddick, H. (1983) Safe-life and damage-tolerant design approaches for helicopter structures. *US Army Research and Technology Laboratories (AVARDCOM).*

[9] Raju, K.S., Smith, B.L., Tomblin, J.S., Liew, K.H., & Guarddon, J.C. (2008). Impact Damage Resistance and Tolerance of Honeycomb Core Sandwich Panels. *Journal of Composite Materials, 42 (4)*, pp. 385 – 412.

[10] Feraboli P. (2006) Damage resistance characteristics of thick-Core honeycomb composite panels. *Proceedings of the 47th AIAA/ASME/ASCE/AHS/ASC Structures, Structural Dynamics, and Materials Conference, Newport, Rhode Island,* 1–4 May 2006, Paper No. AIAA 2006-2169 (American Institute of Aeronautics and Astronautics, Reston).

[11] Lee, I. T., Shi, Y., Afsar, A. M., Ochi, Y., Bae, S. I., & Song, J. I. (2010). Low velocity impact behavior of aluminum honeycomb structures. *Advanced Composite Materials*, *19(1),* pp. 19-39.

[12] Manes A, Gilioli A, Sbarufatti C, Giglio M. (2013). Experimental and numerical investigations of low velocity impact on sandwich panels. *Composite Structures*, *99*, pp. 8–18.

[13] Foo, C.C., Chai, G.B., Seah, L.K. (2006). Quasi-static and low-velocity impact failure of aluminium honeycomb sandwich panels. *Proceedings of the Institution of Mechanical Engineers Part L: Journal of Materials: Design and Applications*, *220,* pp. 53-66

[14] Hazizan, M. A., & Cantwell, W. J. (2003). The low velocity impact response of an aluminium honeycomb sandwich structure. *Composites Part B: Engineering*, *34 (8),* pp. 679-687.

[15] Castanié, B., Bouvet, C., Aminanda, Y., Barrau, J. J., & Thévenet, P. (2008). Modelling of low-energy/low-velocity impact on Nomex honeycomb sandwich structures with metallic skins. *International Journal of Impact Engineering*, *35(7),* pp. 620-634.

[16] Gilioli, A., Sbarufatti, C., Manes, A., & Giglio, M. (2014). Compression after impact test (CAI) on NOMEX™ honeycomb sandwich panels with thin aluminum skins. *Composites Part B: Engineering*, *67*, pp. 313-325.

[17] Crupi, V., Epasto, G., & Guglielmino, E. (2012). Collapse modes in aluminium honeycomb sandwich panels under bending and impact loading. *International Journal of Impact Engineering*, *43*, pp. 6-15.

[18] Zhang, D., Fei, Q., & Zhang, P. (2017). Drop-weight impact behavior of honeycomb sandwich panels under a spherical impactor. *Composite Structures*, *168*, pp. 633-645.

[19] Zhang, D., Jiang, D., Fei, Q., & Wu, S. (2016). Experimental and numerical investigation on indentation and energy absorption of a honeycomb sandwich panel under low-velocity impact. *Finite Elements in Analysis and Design*, *117*, pp. 21-30.

[20] Foo, C. C., Seah, L. K., & Chai, G. B. (2008). Low-velocity impact failure of aluminium honeycomb sandwich panels. *Composite Structures, 85(1),* pp. 20-28.

[21] Jeon, K. W., & Shin, K. B. (2012). An experimental investigation on low-velocity impact responses of sandwich panels with the changes of impact location and the wall partition angle of honeycomb core. *International Journal of Precision Engineering and Manufacturing*, *13(10),* pp. 1789-1796.

[22] Raviprakash, A. V., Prabu, B., & Alagumurthi, N. (2011). Ultimate strength of a square plate with a longitudinal/transverse dent under axial compression. *Journal of mechanical science and technology*, *25(9),* 2377-2384.

[23] Yamashita, M., & Gotoh, M. (2005). Impact behavior of honeycomb structures with various cell specifications—numerical simulation and experiment. *International Journal of Impact Engineering*, *32(1),* pp. 618-630.

[24] Zhao, H., & Gary, G. (1998). Crushing behaviour of aluminium honeycombs under impact loading. *International Journal of Impact Engineering*, *21(10),* 827-836.

[25] Davis, M.J., Chester, R.J., Perl, D.R., Pomerleau, E., Vallerand, M., *Honeycomb Bond and Core Durability Issues; Experiences within CREDP Nations*, Aging Aircraft Conference, Williamsberg, VA, Aug 31-Sep 02 1998.

[26] Tomblin, J. S., Raju, K. S., Liew, J., & Smith, B. L. (2001). Impact damage characterization and damage tolerance of composite sandwich airframe structures. Technical Report. DOT/FAA/AR-00/44.

[27] McQuigg, T. D., Kapania, R. K., Scotti, S. J., & Walker, S. P. (2014). Compression After Impact Experiments on Thin Face Sheet Honeycomb Core Sandwich Panels. *Journal of Spacecraft and Rockets*. *51(1),* pp. 253 – 266.

[28] Aminanda, Y., Castanie, B., Barrau, J. J., & Thevenet, P. (2005). Experimental analysis and modeling of the crushing of honeycomb cores. *Applied Composite Materials, 12(3-4),* pp. 213-227.

[29] Tomblin, J.; Lacy, T.; Smith, B.; Hooper, S.; Vizzini, A.; Lee, S. (1999). Review of Damage Tolerance for Composite Sandwich Airframe Structures. Technical Report, *DOT/FAA/AR-99/49.*

[30] SARISTU – Smart Intelligent Aircraft Structures Project. *AS08 Sensitive coating for impact detection.* Retrieved from the SARISTU website saristu.eu/project/activities/as08-sensitive-coating-for-impact-detection, accessed 19 Oct 2017.

[31] Reyno, T.; Underhill, P. R.; Krause, T. W.; Marsden, C.; & Wowk, D. (2017) Surface Profiling and Core Evaluation of Aluminum Honeycomb Sandwich Aircraft Panels Using Multi-Frequency Eddy Current Testing. *Sensors, 17(9):* 2114

[32] Reyno, T. (2017) *Methods for Characterizing Surface and Core Damage in Aluminum Honeycomb Sandwich Aircraft Panels*. Thesis, Royal Military College of Canada.

[33] Personal communications with members of the Canadian Forces. 2016-2017.

[34] Personal communications with 424 Transport and Rescue Squadron, 8 Wing, Royal Canadian Air Force maintenance personnel. March 2017.

[35] Aktay, L., Johnson, A. F., & Holzapfel, M. (2005). Prediction of impact damage on sandwich composite panels. *Computational Materials Science*, 32(3), pp. 252-260.

[36] Christoforou, A.P., & Yigit, A.S. (1998). Characterization of impact in composite plates. *Composite structures, 43(1),* pp. 15-24.

[37] Christoforou, A.P., Yigit, A.S., Cantwell, W.J., & Yang, F. (2010). Impact response characterization in composite plates—experimental validation. *Applied Composite Materials, 17(5),* pp. 463-472.

[38] Christoforou, A.P., Yigit, A.S., & Majeed, M. (2013). Low-velocity impact response of structures with local plastic deformation: characterization and scaling. *Journal of Computational and Nonlinear Dynamics*, *8(1),* pp. 011012-1 – 011012-10.

[39] Wowk, D., Marsden, C. (2016). Effects of skin thickness and core density on the residual dent depth in aerospace sandwich panels. *International Journal of Computational Methods and Experimental Measurements*, *4*, pp. 336-344.

[40] Horrigan, D. P. W., & Aitken, R. R. (1998). Finite element analysis of impact damaged honeycomb sandwich. *CS503*, *(1),* pp. 1 – 14.

[41] Ashab, A. S. M., Ruan, D., Lu, G., & Bhuiyan, A. A. (2016). Finite element analysis of aluminum honeycombs subjected to dynamic indentation and compression loads. *Materials*, *9*(3), 162.

[42] Fan, X. L., Wang, T. J., & Sun, Q. (2011). Damage evolution of sandwich composite structure using a progressive failure analysis methodology. *Procedia Engineering*, *10*, pp. 530-535.

[43] Ramberg, W., & Osgood, W. R. (1943). Description of stress–strain curves by three parameters. Technical Note No. 902, National Advisory Committee For Aeronautics, Washington DC.

[44] Nguyen, M. Q., Jacombs, S. S., Thomson, R. S., Hachenberg, D., & Scott, M. L. (2005). Simulation of impact on sandwich structures. *Composite Structures*, *67(2),* pp. 217-227

[45] Staal, R. A. (2006). *Failure of sandwich honeycomb panels in bending* (Doctoral dissertation, ResearchSpace@ Auckland).

[46] Horrigan, D. P. W., & Staal, R. A. (2011). Predicting Failure Loads of Impact Damaged Honeycomb Sandwich Panels-A Refined Model. *Journal of Sandwich Structures & Materials*, *13(1),* pp. 111-133.

[47] Schubel, P. M., Luo, J. J., & Daniel, I. M. (2007). Impact and post impact behavior of composite sandwich panels. *Composites Part A: applied science and manufacturing*, *38(3),* pp. 1051-1057.

[48] Engineering Virtual Organization for CyberDesign. (2015). SSC Aluminum: Al 7075-T6 alloy [Materials property database] Retrieved from icme.hpc.msstate.edu/mediawiki/index.php/SSC_Aluminum:_Al_7075-T6_alloy, accessed 12 June 2017.

[49] Callister, W. D., & Rethwisch, D. G. (2011). *Materials science and engineering* (Vol. 5). NY: John Wiley & Sons.

[50] James, C. T., Watson, A., & Cunningham, P. R. (2015). Numerical modelling of the compression-after-impact performance of a composite sandwich panel. *Journal of Sandwich Structures & Materials*, *17(4),* pp. 376-398.